DYNAMIC MODELLING AND CONTROL SCHEMES FOR CURRENT- SOURCE RESONANT CONVERTERS

Thesis submitted in partial fulfillment of the requirement for the PhD Degree issued by Polytechnic University of Catalonia, in Electronic Engineering Program.

Mohammad Moradi Ghahderijani

Director: Dr. Miguel Castilla Fernández
Co-director: Dr. Jaume Miret Tomàs

2018

"If you have no sympathy for human pain
The name of human you cannot retain"

Saadi Shirazi *(1210-1291) - Persian Poet*

Summary

This thesis focuses on the control methods applied to current source resonant converters, especially in two different applications of switching power supplies and wireless power transfer systems. In fact, the existing applications are mostly working with voltage source resonant converters. For voltage-source resonant converters, many control strategies have been analyzed and investigated, turning this into a mature technology nowadays. The current-source resonant converter is an alternative solution as they offer well-known advantages such as non-pulsating input current, low stress for switches, simple driving circuitry, and short circuit protection capabilities.

However, there is an obvious lack of control methods applicable to current-source resonant converters. In addition, obtaining an appropriate dynamic model to be used in control design is the other challenging issue in this field. Hence, the objectives of this thesis are used to fill these gaps. The proposed control schemes are:

- Frequency modulation control scheme applied to a DC/DC current-source parallel resonant converter.
- Sliding mode control scheme with amplitude modulation applied to a DC/DC current-source parallel resonant converter.
- A control scheme for a multiple-output DC/DC current-source parallel resonant converter.
- A communication-less control scheme for a variable air-gap wireless energy transfer system using a current-source resonant converter.

Resumen

Esta tesis doctoral está centrada en los métodos de control aplicados a los convertidores resonantes con fuente de corriente, especialmente en dos aplicaciones distintas como son fuentes de alimentación conmutadas y sistemas de transferencia de energía sin hilos. De hecho, las aplicaciones existentes trabajan principalmente con convertidores alimentados mediante fuentes de tensión. Hasta hoy en día, en la literatura especializada se han analizado muchas estrategias de control para convertidores resonantes con fuente de tensión, lo que hace que esta sea una tecnología madura. El convertidor resonante con fuente de corriente es una solución alternativa, que ofrece ventajas conocidas como corriente de entrada no pulsante, bajo estrés para los interruptores, circuitos de disparo sencillos y protección contra cortocircuitos.

Sin embargo, existe una falta evidente de métodos de control aplicables a los convertidores resonantes con fuente de corriente. Además, otro desafío en este tema es la obtención de modelos dinámicos apropiados para el diseño del control. Por lo tanto, los objetivos de esta tesis se utilizan para llenar estos vacíos. Los esquemas de control propuestos son:

- Esquema de control en frecuencia aplicado a un convertidor resonante paralelo con fuente de corriente para reguladores de tensión en continua.
- Esquema de control en modo de deslizamiento con modulación de amplitud aplicado a un convertidor resonante paralelo con fuente de corriente para reguladores de tensión en continua.
- Esquema de control para un convertidor resonante paralelo con fuente de corriente para la regulación de tensión en continua de varias salidas.
- Esquema de control sin comunicaciones para un sistema de transferencia de energía sin hilos con un transformador con entrehierro variable basado en un convertidor resonante con fuente de corriente.

Acknowledgment

This thesis has been carried out at Technical University of Catalonia (UPC), Barcelona, Spain, at the laboratory of Power Electronics and Control Systems (PECS) group. This work would have been difficult to finish without the guidance and the help of several individuals.

I would like to first express my special thanks of gratitude to my supervisor Dr. Miguel Castilla as well as my co-supervisor Dr. Jaume Miret for their continuous support to my Ph.D study and related researches.

I would also like to thank Prof. Luis Garcia de Vicuña and my other friends in PECS laboratory (Antonio, Ramon, Javi Torres, Arash, Javi Morales, Juan, Miguel Garnica). It was fantastic to have the opportunity to work majority of my research with this group. What a cracking place to work!

A very special gratitude goes out to all my family members, with a special mention to my parents and siblings, those who encouraged me to study PhD abroad and finally my wife for her company and patience during these years.

Contents

Chapter5

Chapter6

CHAPTER 1

Introduction

Summary

This chapter introduces the concept of resonant converters. From a historical review to the description of the typical applications, the chapter classifies the resonant converters according to their topologies and the commonly-used switching networks for each topology. Likewise, a problem formulation is presented in order to highlight the present unsolved problems for each application. Moreover, the main objectives of this thesis is also presented.

1.1. HISTORICAL BACKGROUND AND CURRENT STATUS

Conventional pulse-width modulated (PWM) converters [l]-[5] are well studied in the literature and are still widely used as a part of low and medium-power applications. However, the turn-on and turn-off losses caused by PWM rectangular voltage and current waveforms limit the operating frequency and produces hard switching. This yields in power losses and electrical stress in switches. Furthermore, hard switching leads to sharp changes of voltage and current (dv/dt and di/dt) that are the major source of broad-band electromagnetic energy and thus increase the potential for electromagnetic interference (EMI). The inefficient operation of PWM converters at very high frequencies imposes a limit on the size of reactive components of the converter and consequently, on power density.

The adverse effects of hard switching – i.e., power losses, electrical stresses, and EMI – are more and more important as the switching frequency increases. Several papers have studied the effects of hard switching [6] along with circuitry arrangements to modify the current and voltage at the switches during the commutations to eliminate or at least mitigate its effects [7], [8]. These proposals are based on circuitry that forces at zero either the voltage across the switches (ZVS) when they are turned on, or the current through the switches (ZCS) when they are turned off, or both. In addition, the converters with the switches commutating in such a soft way are called soft-switching converters [9]. The principle of operation and design of these converters are widely studied in the literature [10]– [11] for both ZVS and ZCS converters. Switching losses, electrical stresses on the devices, and EMIs are significantly decreased in these soft-switching converters. The loss decrease can be utilized to raise the working frequency of the converters, when permitted by the application. This allows a reduction in the size of the magnetic components of the converters, such as transformers and passive filters.

Basically, depending on the operating principle, soft switching converters are categorized in three different families 1) quasi-resonant converters and multi-resonant converters, 2) resonant-transition converters, and 3) resonant converters. The general schematic of these converters is shown in Fig. 1.1.

Fig. 1.2. shows the details of various types of soft-switching converters. As shown in Fig. 1.2.(a) and Fig. 1.2.(b), the quasi resonant converters are built by inserting reactive elements in a hard-switching converter. To ensure soft switching, two auxiliary devices composed of

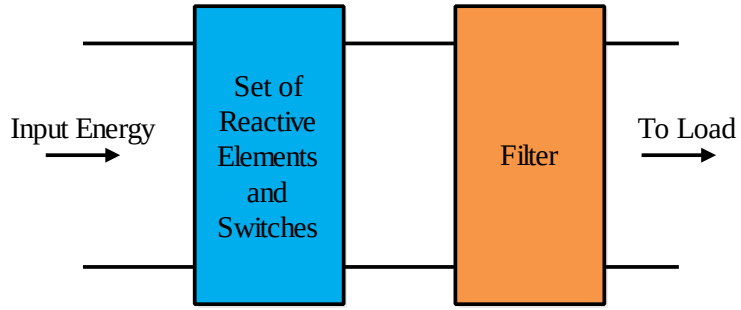

Fig. 1.1. General diagram of a typical soft-switching converter

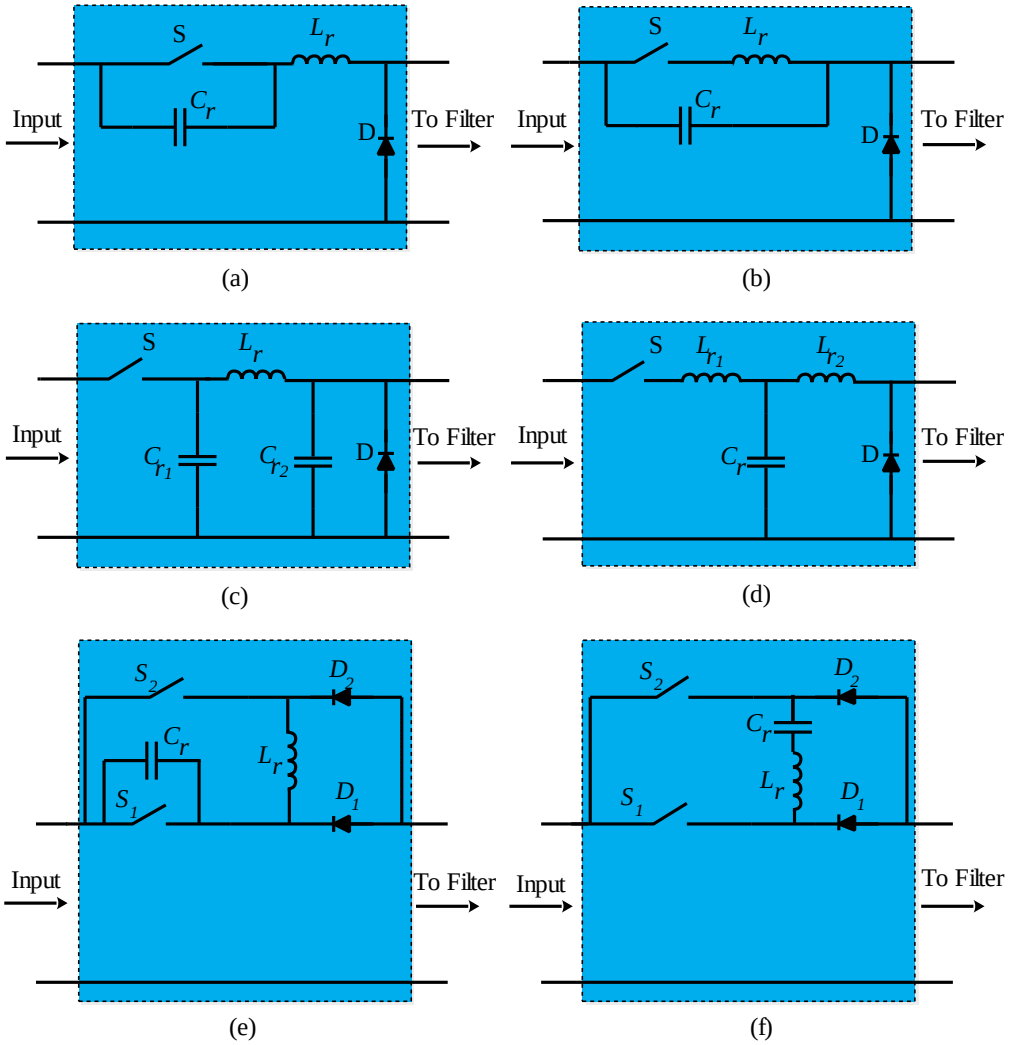

Fig. 1.2. Schematic diagram of (a) ZVS quasi resonant converter, (b) ZCS quasi resonant converter, (c) ZVS multi resonant converter, (d) ZCS multi resonant converter, (e) ZVS resonant-transition converter, and (f) ZCS resonant-transition converter

reactive elements of different kinds (L_r, C_r) are used in these converters, while in multi-resonant converters, three reactive elements are normally used [12], as shown in Fig. 1.2.(c) and Fig. 1.2.(d). The principle of operation and characteristic analysis of these group of

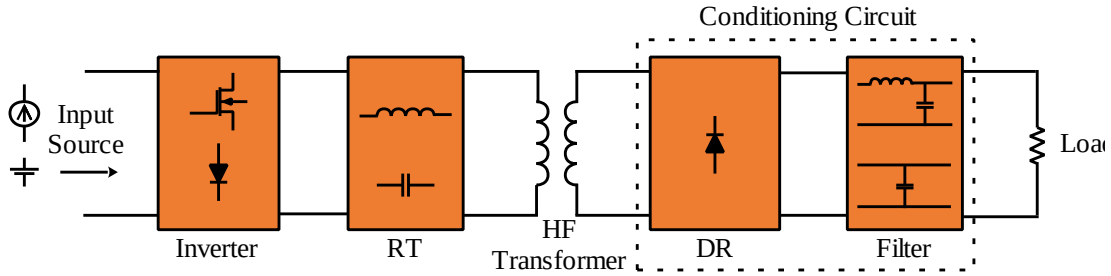

Fig. 1.3. Schematic diagram of resonant converters

converters are well studied in [13], [14]. These converters have been applied in induction cooker [15] and induction heating [16] applications.

To achieve soft switching in resonant-transition converters four auxiliary devices including two reactive elements of different kinds and two auxiliary switches are applied, as shown in Fig. 1.2.(e) and Fig. 1.2.(f). During commutation, either zero-voltage transition or zero-current transition can be obtained. The characteristics of these converters was investigated in [17], [18].

To work as a soft-switching converter, the third family, i.e., resonant converters, follow a quite different method: inserting the auxiliary devices in cascade with the converters instead of connecting them around the switches [19]. The structure of these converters is shown in Fig. 1.3. The input inverter takes the energy from a dc source and generates a high frequency ac voltage or current, depending on the input source type.

The task of the resonant tank (RT) is to provide the resonance conditions for the voltage/ current across/ through switches of the input inverter to ensure a soft commutation. The RT output supplies the conditioning circuit (CC) that delivers energy to the load. The CC contains a unidirectional converter normally a diode rectifier (DR) when no inversion of the power flow is required; otherwise it contains a bidirectional converter. Finally, the CC contains a filter, low-pass (LPF) or band-pass (BPF), used to meet the power quality required by the load. The inductive or capacitive kind of filter defines the current- or voltage sink nature of the load. Between the input stage and the CC, resonant converters often include an HF-transformer either to change the input-to-output voltage level or to assure an input-to output galvanic isolation.

Nowadays, among the mentioned soft switching converters, resonant converters are more interesting due to their high performance in terms of power density and efficiency [19]. In addition, resonant converters have wide input and output voltage range characteristics, their

output voltage and current present low ripple, and they do not require a complicated filter design [19]. Hence, this thesis focuses on them.

1.2. RESONANT CONVERTER TOPOLOGIES

The arrangement of different types of stages (input source, inverter, RT, and even the output filter) determines the features of a resonant converter topology. Of course, the various stages must be compatible with each other. A typical resonant converter can be generalized based on four different input source and output sink excitations as listed below [19]:

- Voltage source/Voltage sink (V-V)
- Voltage source/Current sink (V-C)
- Current source/Voltage sink (C-V)
- Current source/Current sink (V-V)

1.2.1. Input source topologies

As a whole, depending on the characteristic of the input source, resonant converters are divided into two categories of voltage and current source converters. Unlike voltage source resonant converters, in current source ones, a choke inductor must be inserted in series with the input voltage source to get a practical current source.

In voltage source resonant inverters, the shape of the current injected to the resonant tank is a sinusoidal waveform. in current source resonant inverters, the current drawn from the dc voltage supply is constant and continuous, leading a square shape current to be injected to the resonant tank. The reason is that the choke inductance value is much larger than the resonant inductor, so under normal steady-state operation the input current is approximately constant.

1.2.2. Switching network topologies

For current-source resonant converters, taking into account the input converter, different main switching topologies have been investigated, as detailed in the next subsections. Note that since the focus of this thesis is on the current source converters, the voltage source switching networks are not presented.

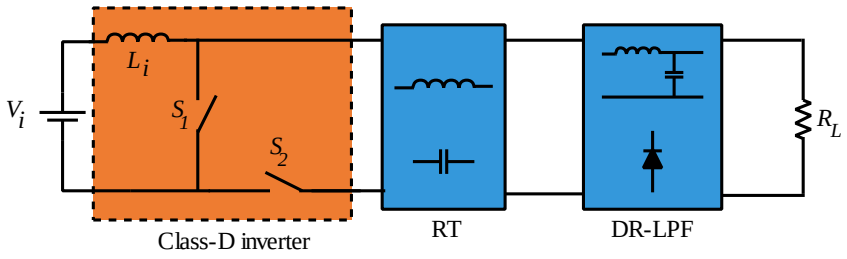

Fig. 1.4. Circuit diagram of Class D current source resonant converter

1.2.2.1. Class D topology

As can be seen from Fig. 1.4, the class D switching topology is composed of two switches which both are driven with respect to the ground, therefore make the driving easy [23]. The switches are driven by a rectangular signal at the operating frequency and with a duty cycle of slightly higher than 50%. To provide a path for the dc input current, either one or both switches should be ON. Therefore, a slightly overlapping in the ON states of both switches should be used to obtain the simultaneous conduction of switches. When the switch S_1 is OFF and S_2 is ON, input current flows through the resonant tank. Therefore, energy will be transferred from dc input source to the resonant tank. On the contrary, if *S1* is ON and *S2* is OFF, the input current passes through S_1 and the energy is kept in the resonant tank is partially discharged to the load.

1.2.2.2. Full-bridge topology

In this topology like previous one, the inductance of input inductor is much larger than the resonant inductor, so under normal steady-state operation the dc-link current is approximately constant and the inverter injects a square-wave current, into the resonant tank through *S1–S4* and *S2–S3* [23]. In this circuit as illustrated in Fig. 1.5, this current is injected to the parallel load and return to the source when switch *S1* and *S4* are ON on the half of the period *T* ($0<t<T/2$). This process repeats for *S2* and *S3* during second half period ($T/2<t<T$). Note that, the peak current of each switch is the same as in the Class-D switching topology. On the other hand, in full bridge topology, the switching is more complex as a result of floating source pins of the top switch.

1.2.2.3. Push-pull topology

The circuit diagram of a typical push-pull current source resonant converter is depicted in Fig. 1.6. As shown, the current of L_2 is injected to the parallel load and return to the source

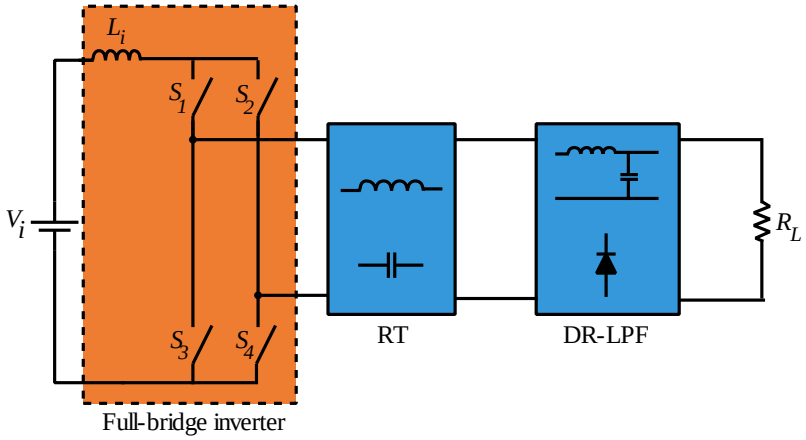

Fig. 1. 5. Circuit diagram of full-bridge current source resonant converter

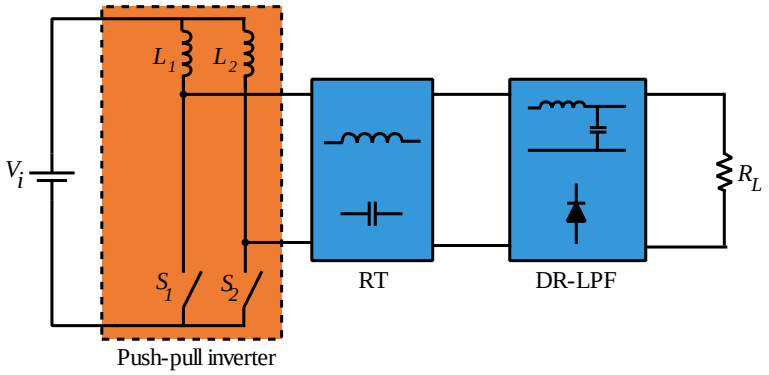

Fig. 1.6. Circuit diagram of push-pull current source resonant converter

when switch *S1* is ON (*0<t<T/2*). This process repeats for *S2* during the second half period (*T/2<t<T*). In this topology, the current injected to the resonant tank is half of the current in Class-D topology (considering a same power rate). Therefore, this topology is recommended for some special applications, for instance in residential inductive contactless energy transfer systems. In this application, this current follows through the primary side cable, so a noticeable reduced power loss can be ensured by using push-pull topology [24]. On the other hand, in comparison with full bridge topology, the main difference refers to that a phase splitter (two input inductors instead of one) used in the push-pull inverting network. This topology changes the ratio between input voltage and the resonant voltage. In steady state, as the average voltage of the input inductor is zero, the average resonant voltage of the full bridge topology is equal to the input voltage. But for the push-pull topology, the completely coupled phase splitter: equally divides the resonant voltage, so its resonant voltage doubles that of the full bridge topology. Thus, the push-pull topology is more suitable for applications that require a higher resonant voltage for a limited input voltage. Another advantage of the push-pull topology is that both switches are grounded. The other advantage of the push-pull

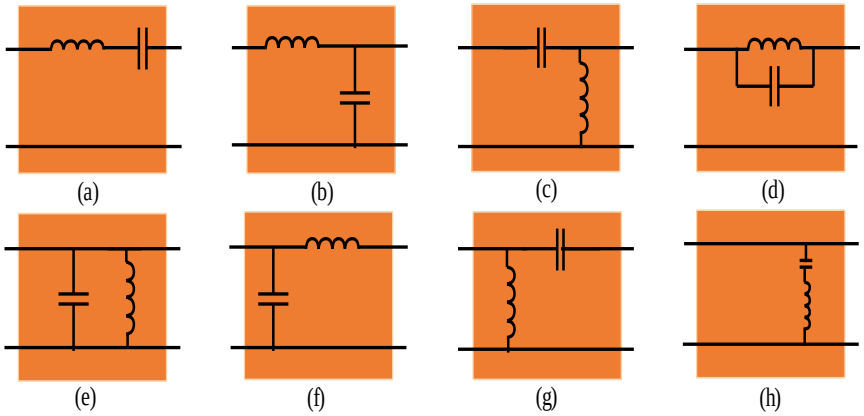

Fig. 1.7. Two-element RT combinations

method is the reduction in the number of switches in comparison with the full bridge topology.

1.2.3. Resonant tank

The number of elements for a RT and their configuration also differentiates the topology. The more elements in an RT, the more topologies that can be obtained. However, not all the combinations of the elements produce a resonant condition. According to the analysis in [20], for an RT with two elements, there are eight possible topologies, with three elements there are 36, with four elements there are 182, and with five elements there are several hundred possible topologies.

Two-element RT is the simplest of various possible configurations. All possible circuit combinations for second-order resonant tank is shown in Fig. 1.7. As already mentioned, not all the combinations can provide resonant condition. Hence, these combinations are classified as below:

- Resonant Coupled converter topologies (R)
- Non-resonant Coupled converter topologies (N)
- Unrealizable converter topologies (U)

Based on the analysis done in [20], following rules of thumb can be concluded:

- When a current source is in series with a capacitor, the resultant topology is non-resonant coupled;
- When a voltage source is in parallel with an inductor, the resultant topology is also non-resonant coupled;
- The dual of a resonantly coupled topology is also resonantly coupled;

Table.1.1. Classification of the second order resonant tank topologies

Source/Sink	R converters	N converters	U converters
V-V	a, h	-	Other 6 combinations
V-C	d, c, b, h	g	Other 3 combinations
C-V	d, h, f, g	c	Other 3 combinations
C-C	d, e	-	Other 6 combinations

Table. 1.2. Number of resonant topologies

Resonant Converters	V-V	V-C	C-V	C-C
3rd order	6	7	7	6
4th order	17	44	-	-

- The dual of a non-resonantly coupled is an unrealizable topology.

Table 1.1 classifies all topologies given in Fig. 1.4, for different combinations of input and output excitations.

Applying the mentioned rules to the higher order resonant tanks, Table 1.2 determines the number of topologies which provide resonant condition.

1.2.4. Output sink

The dc output voltage sink or current sink are typically implemented by using a diode rectifier DR circuit in order to rectify and couple the resonant current or voltage from resonant tank to the output circuit. The output circuit also consists of a LPF of either capacitive or inductive type. Fig. 1.8 and 1.9 show the voltage and current waveforms characterizing the DR–LPF set, with RT current and voltage output and, respectively, capacitive and inductive LPF.

1.2.5. Examples

1.2.5.1. V-V series resonant converter

The topology of Fig. 1.10 leads to the well-known voltage source-voltage sink series resonant converter (SRC), one of the oldest and most widely presented in the literature [21], [22]. The topology stands out due to the fact that both elements are in series with the load.

Consequently, as the load increases, the current through the RT and inverter switches decreases and vice versa. Due to its current filtering, the RT delivers a sinusoidal current, and the DR–LPF set must be of a capacitive nature. Voltage and current waveforms involved in the DR–LPF circuit of the SRC are shown in Fig. 1.8.

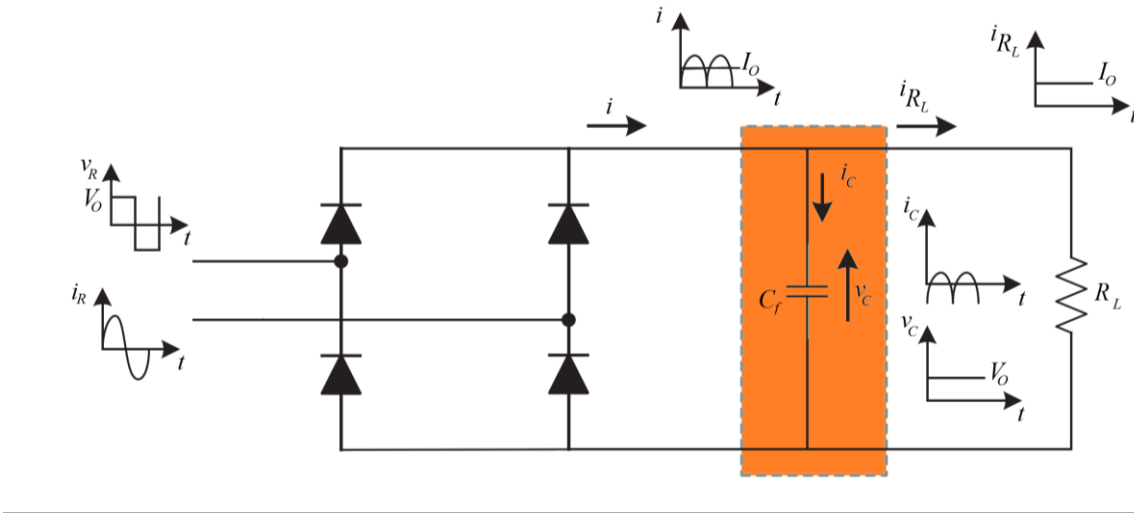

Fig. 1.8. The voltage and current waveforms of a capacitive LPF.

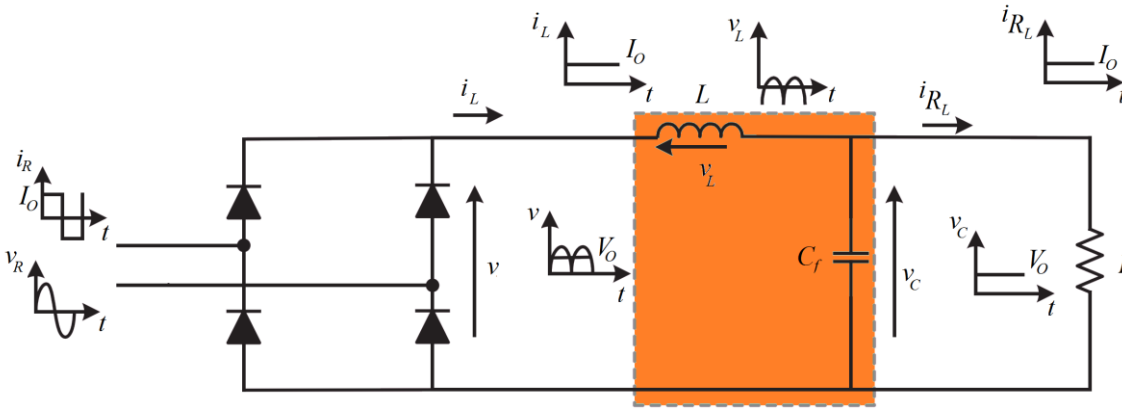

Fig. 1.9. The voltage and current waveforms of an inductive LPF.

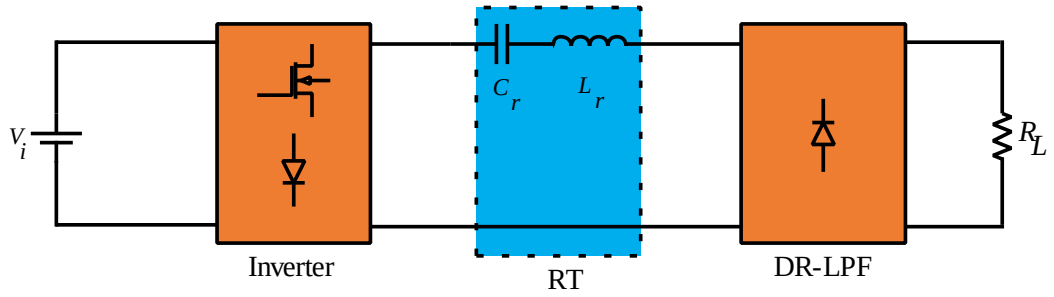

Fig. 1.10. V-V SRC circuit diagram

1.2.5.2. C-C parallel resonant converter

The parallel resonant converter (PRC) topology of Fig. 1.11 differs from the SRC topology in two points: 1) the resonant capacitor C_r and inductor L_r are in parallel with the

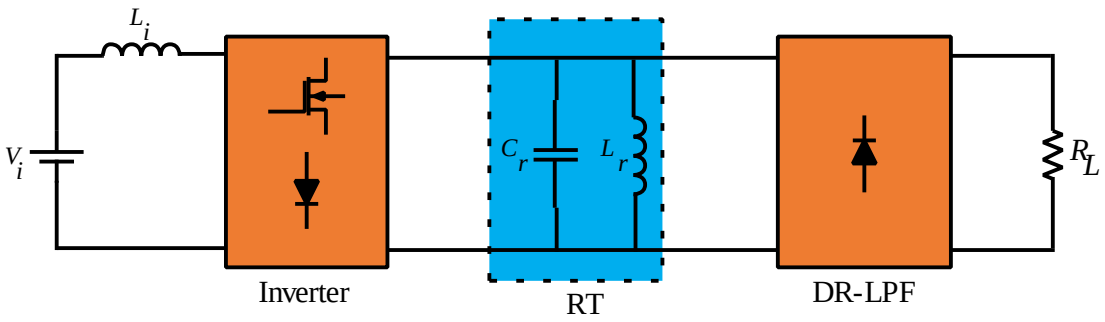

Fig. 1.11. C-C PRC circuit diagram

DR and, hence, with the load, and 2) the DR has an in-cascade inductive LPF. Moreover, the voltage across the resonant tank increases as the load decreases. Due to its voltage filtering, the RT delivers a sinusoidal voltage and the DR–LPF set must be of an inductive nature. Voltage and current waveforms involved in the DR–LPF circuit of the PRC are shown in Fig. 1.9.

1.3. MODES OF OPERATION

Generally, a resonant converter can be operated in two different modes: continuous and discontinuous modes. As a whole, the ratio of switching frequency to resonant frequency determines the mode of operation [25]. In series resonant converter, this ratio decides if the input current of the resonant tank flows continuously or discontinuously. However, in parallel resonant converters, instead of resonant current, its voltage has the continuous or discontinuous property.

1.3.1. Discontinuous mode

This mode of operation occurs both above and below resonance when switching frequency is less than the half of the resonant frequency or more than twice. This mode occurs when the load of the converter is low.

A discontinuous conduction mode mechanism can occur in the parallel resonant converter. In this mode, a discontinuous subinterval occurs in which all four output bridge rectifier diodes are forward-biased, and the tank capacitor voltage remains at zero. Due to its high conduction losses, it is not the preferred mode of operation.

1.3.2. Continuous mode

This mode of operation is also divided in two sub-modes: leading and lagging power factor.

1.3.2.1. Continuous conduction mode with leading power factor

If RT presents capacitive input impedance, resonant current leads the voltage across the resonant tank. This mode is not also the preferred mode of operation for neither series nor parallel resonant converter. For example, for parallel resonant converter, in this mode, the switches of the input inverter experience soft switching and zero turn-off switching loss and the series diodes experience zero turn-on switching loss. However, there is turn-on switching loss in each switch and reverse-recovery turn-off loss in each series diode. For these two reasons, the efficiency in this case is less than that with lagging power factor.

1.3.2.2. Continuous conduction mode with lagging power factor

If RT presents inductive input impedance, resonant current lags the voltage across the resonant tank. This mode is the preferred mode of operation for both series and parallel resonant converters. Note that, in this case, the series resonant converter works in above resonance (switching frequencies slightly higher than resonant frequency), while the parallel resonant converter works in below resonance (switching frequencies slightly lower than resonant frequency).

1.4. MODES OF CONTROL

The control strategy has been one of the challenging research keys in resonant power converters. For voltage source series resonant converters, many control strategies have been analyzed and investigated [26] - [31], turning this into a mature technology nowadays. Some of these control techniques are briefly explained in this Section.

1.4.1. Phase modulation control

The basic idea behind this modulation technique is to apply a change in duration of the zero interval of the RT input voltage in order to reach the output voltage value required by the application. This technique was introduced to control the SRC in [23]. An extension to the series-parallel resonant converter was presented in [26].

1.4.2. Quantum modulation control

The main concept behind this technique is to force the switching network to follow the resonant frequency and change the state of the switches exactly at the zero-crossing of the current or voltage, depending on the topology i.e., voltage or current source one. This method

has been treated extensively to voltage source resonant converter in for example [27] and [28].

1.4.3. Frequency modulation control

The fundamental concept behind this technique is to adjust the output voltage via changing the switching frequency. This controller has been widely applied to the voltage source resonant converter [24].

1.4.4. Clamped Mode Control

The clamped mode (CM) operation is possible with full-bridge resonant converter circuit and was developed as the functional equivalent of phase controlled resonant converters. In this method, output voltage is controlled by phase-shift pulse width modulation.
The CM control, complete steady state analysis, investigation of different operating modes and mode boundaries has been extensively reported for SRC [29], and a three-elements resonant tank topology [30].

1.4.5. Self-Sustained Oscillating Control

The phase angle between the bridge output voltage and current can be controlled for ZVS operation by generating the bridge output voltage and by sensing the phase of the current. In this case, the converter is said to be operating in so called self-sustained oscillating mode [31], [32].

1.4.6. Control strategies applied to current source resonant converter

In [33], a simple modulation technique has been proposed for this type of converter and then applied to an induction heating system [34]. This method is then further developed in [35]. In [36], the modulation technique has been applied to an inductive contactless energy transfer system. A delta-sigma modulator is also applied to a class-D current-source parallel resonant converter (CSPRC) in [37]. In all these works, the current-source converters operate in open loop and thus they exhibit a high sensitivity to external disturbances and parameter variations.

1.5. APPLICATIONS

Resonant converters are more often used in emerging applications due to the mentioned advantages in Section 1.1. This subsection gives an overview of the most significant

technology areas where resonant converters are being researched and applied. Some of this applications are power supplies, electric and plug-in hybrid vehicle charging through either wired or wireless power transfer, grid-connected converters of renewable energies such as photovoltaic (PV), wind, and fuel cells, and induction cookers.

1.5.1. Power supplies

The main requirements for power supplies of electric equipment are high reliability, high efficiency, small size, long life, and low cost [38]. The technical solution devised to set up a highly efficient power supply is soft switching, which is implemented through on-purpose developed power circuitry, i.e., by resonant converter. The topology selection depends on parameters such as output power, input voltage, and the output/input voltage ratio. The selection of the topology also influences the size, price, and efficiency of the power supply, which is one of the most important challenges of its design.

1.5.2. Electric and plug-in Hybrid Vehicle Charging

By 2020, more than half of new-vehicle sales are expected to be electric vehicle (EV) models [39]. The enabling technology to this revolutionary change is the battery. Charging the batteries of electric and plugin hybrid vehicles can be done by wire or wirelessly. Although a wired battery charger has the advantage of exploiting a rather simple and well-grounded technology, it obliges users to fumble with cables and plugs, even under adverse weather conditions or while they are hindered by bags, parcels, and so on. With wireless power transfer (WPT) technology, EV charging is more user friendly and opens the possibility of recharging vehicles while they are running, thus solving the problem of the short range achievable with currently available batteries. The inductive WPT systems to charge EV battery packs have been growing in recent times due to their advantages with respect to their wired counterpart [42]. Therefore, WPT charging is playing a major role in EV charging. Several WPT technologies such as electric, magnetic, and electromagnetic are available. However, technologies using magnetic coupling with resonant circuits offer the highest power transfer efficiency and higher wireless transmission power at near-field distances. In the transmitter section, a high-frequency resonant inverter feeds the transmitting side of the coil coupling. This encompasses a transmitting coil, a reactive power compensating network formed by one or more capacitors, and possibly inductors that are connected in series and/or in parallel. The transmitting coil generates a variable magnetic flux that links the receiving coil and induces an alternate voltage across its terminals. The receiving side of the coil

coupling in turn encompasses the receiving coil and another reactive power compensating network. The induced voltage, once conditioned by a receiving rectifier and a chopper, is applied to the EV battery pack to charge it. Consequently, the use of resonant converter circuits in the transmitter and the receiver sections allows for maximizing the magnetic field coupling and achieves the highest power transfer capability at the resonance frequency. Several resonant converter topologies for charging electric and plug-in hybrid vehicles are documented in the literature, both in the wired [39]–[41] and WPT [42]–[44] modes.

1.5.3. Renewable Energy sources and Their integration into the Grid

Renewable energy technologies have been recognized as the most effective solutions to the increasingly serious energy crisis and environmental pollution. Overall, in renewable and alternative energy sources such as photovoltaic, wind, and fuel cells, the output voltage varies over a wide range with climate, weather, and operational conditions. On the other hand, small current ripple and high power conversion efficiency are usually required for long-term, reliable, and efficient operation. Integration of these sources into the grid with high efficiency is the major research area where power electronics converters and their controls play a critical role. DC/DC converters are usually the front-end stage of integration of renewable energy into the grid, and they need to be highly efficient to enhance the overall system. Among the various possibilities for the dc/dc converter, resonant converters have been attracting more attention due to their aforementioned inherent merits. As a result, resonant converters are used in electrolyzers [45], PVs [46], fuel cell systems [47], [48], and interfaces with the grid [49], [50].

1.5.4. Induction Cookers

Domestic induction cookers (also known as induction heaters) have become very popular today due to advantages such as efficiency, fast heating, cleanliness, and safety. To achieve high efficiency, induction cooktops usually feature resonant converters in which the inductor-vessel system is a part of the resonant tank. Thus, the inductor vessel system impedance sets the point of operation of the power converter. Due to the variability of the load, with multiple parameters such as temperature, geometry, and material, the resonant converters must work with highly variable operating conditions. The energy is first filtered electromagnetically to fulfill the EMC regulations; then, by a rectifier and a filter, the AC mains voltage is converted to a DC bus; and finally an inverter converts the bus voltage into

a medium-frequency AC current that flows through the inductor coil, heating up the vessel. Improvements in this field by the adoption of resonant converters are presented in [51]–[53].

1.6. STATE OF THE ART CHALLENGES

As mentioned in previous sections, voltage-source converters have been widely analyzed and investigated, turning this into a mature technology nowadays. However, the profits of the current-source resonant converter have made it a better option to apply the enhanced features of resonant converters to practical applications, ranging from low to high power.

On the other hand, compared to the series resonant topologies, parallel resonant converters absorb a continuous smooth current from the input source, offering low current stress to switches [23]. Likewise, the reactive power circulates inside the parallel resonant tank and only the active power is supplied through the switches. This feature provides the capability of generating high current and voltage levels by using low VA-rated switches, reducing conduction losses. In addition, these converters provide more facilities such as simple driving circuitry, short-circuited protection and paralleling capabilities. Note that short-circuit ability is important in applications where short-circuit is happening on the load from time to time. So this ability is essential in protecting system from breaking down. For the reasons outlined above, the research on the current source resonant converters has recently attracted more interest [33]-[37].

In this thesis, the application of current source resonant converters on DC/DC converters as switching power supplies and wireless energy transfer system is investigated. To do this, in this Section, the challenges in each application is first presented.

1.6.1. DC/DC converter

DC-DC conversion category is an industry example of great importance for resonant converters. Battery charging, electronic air purifiers, and switching power supplies are among these applications, ranging from low to high power [54]-[55].

The functions of DC-DC converters are as follows:

- To convert a DC input voltage V_i into a DC output voltage V_o;
- To regulate the DC output voltage against load and line variations;
- To reduce the AC voltage ripple on the DC output voltage below the required level;
- To provide isolation (if required) between the input source and the load;
- To protect the supplied system from electromagnetic interference (EMI);

• To satisfy various international and national safety standards.

A great interest has been taken in resonant converters due to their generated high frequency sinusoidal waveforms, reducing the electromagnetic interference and switching losses [56]. The control strategy has been one of the challenging research keys in this field. For voltage-source resonant converters, many control strategies have been analyzed and investigated [26]-[31], turning this into a mature technology nowadays. However, due to the reasons stated in previous section, the research on the current source ones has recently attracted more interest [33]-[37]. In this field, the current-source converters operate in open loop and thus they exhibit a high sensitivity to external disturbances and parameter variations. So, there is a need to find a closed loop control system to cover all the mentioned issues in this field.

1.6.2. Wireless energy transfer system

During the last decade, WPT systems have attracted remarkably interest on industry sectors such as smartphone charging platforms, electric vehicle charging, and medical implants [57]–[59]. This technology has created new possibilities to transfer electrical energy in a spark-less way and with no electric shock hazard. In these works, the air gap has been considered constant while in certain applications using WPT systems, it is not possible to assume working conditions in which the length of the air gap would remain unchanged, e.g. charging of electric vehicles [63], [64]. This condition yields in a variation in magnetic coupling and even circuit parameters. This problem from one-side and load variations from the other side lead to a resonant frequency drift in the contactless system and the output voltage differs from its main reference value. This issue causes challenges especially in applications where a constant regulated output voltage is required. To avoid this problem and to have a soft switching, i.e., to ensure ZVS, some compensation topologies and control mechanisms have been explored in the literature [65], [66]. Normally, to have a good control in the receiver circuit, a feedback control is required. The typical control method in this case is primary-side control. In this method, some information from the secondary side of the transformer are directly sensed and sent to the primary control system via wireless communication networks [67], [68]. The other conventional way is to estimate the mutual coupling between two coils of the transformer [69]. With this estimation, the output voltage can be indirectly calculated and used in the closed-loop control. But the estimation is based on the nominal component values. Hence, this method is not accurate due to the tolerance of the components and the temperature effect during operation.

1.7. RESEARCH OBJECTIVES

In this section the main objectives of this thesis are introduced. The main focus of this thesis is the application of current source resonant converter in DC/DC converters and wireless energy transfer systems. According to the mentioned problems, several challenges are identified which will be address in this thesis.

1.7.1. Dynamic model for the current source parallel resonant converter

The first issue missed in literature is introducing the mathematical formulation of the system, i.e. mathematical equations of the current source resonant converter. Therefore, the first open topic is to derive an averaged circuital model for the system which allows us to describe the dynamic behavior of the converter. This model will be used for designing the controller and its parameters.

1.7.2. Designing a closed loop control for CSPRC

The next topic is to design and compare different closed loop controls for the current source resonant converter based on different modulation techniques. As mentioned in previous section, there are some modulation techniques to govern a current source parallel resonant converter. But majority of them are working in open loop. Therefore, in this thesis what is more interesting and also critical for the system is to find a closed loop robust control approach to overcome all the constraints associated with the control objectives. For example, one of the purposes is a strategy to simultaneously fix the output voltage, while ensuring ZVS condition and with a fast transient response.

1.7.2.1. Frequency-Modulation Control of a DC/DC Current-Source Parallel-Resonant Converter

The first control scheme introduced in this thesis is based on the frequency modulation technique for the DC/DC Class-D CSPRC intended for switching power supplies. This control is responsible for both regulating the output voltage and providing zero voltage ZVS conditions as the main control objectives. On the other hand, once, the dynamic model for the closed-loop system is formulated, a systematic procedure to design the control gains is also necessary.

1.7.2.2. Robust and Fast Sliding-Mode Control for a DC-DC Current-Source Parallel-Resonant Converter

Sliding-mode control offers robust operation and fast transient response. The next aim of this thesis is to propose a robust sliding-mode control with a fast transient response for a DC-DC current-source parallel-resonant converter. This control scheme is based on an amplitude modulation technique. The idea is to fulfill all objectives mentioned in previous subsection.

1.7.3. Control Scheme for a Multiple-Output DC/DC CSPRC

The next purpose of this thesis is to present a proper control scheme for a multiple-output DC/DC class-D CSPRC. In order to charge electric devices such as laptop PC and smart phone or other electronic loads without using AC adapters, a simple and low cost DC/DC converter using a multi-output current source resonant converter is proposed.

The idea is to extend all the theoretical parts of the single-output converter in previous subsection for a multiple-output converter. To do this, the theoretical analysis must include the derivation of the averaged large-signal model and the synthesis of the control scheme. The control scheme is responsible for both regulating the output voltage and providing ZVS condition in all different operation conditions including load step changes or resonant parameter variations.

1.7.4. A Communication-less Control Scheme for a Variable Air-gap Wireless Energy Transfer System using Current Source Resonant Converter

The last aim of this thesis is to propose a robust control method for a variable air-gap wireless energy transfer system using current source resonant converter 1) to provide a constant output voltage, 2) to track the resonant frequency, and 3) to ensure ZVS condition, regardless of any changes in system parameters or/and load variations. In this method, there is no need to use neither a wireless communication system nor mutual coupling estimation.

1.8. STRUCTURE OF THE THESIS

This thesis has been written as a compendium of publications, including 4 papers that present the most relevant works in the field of research.

The structure of the thesis is divided into 3 major parts:

- Introduction (Chapter 1)
- Publications (Chapter 2, 3, 4 and 5)
- Analysis of the results (Chapter 6) and Conclusions (Chapter 7)

The first part of the thesis is the introduction (Chapter 1). This part of the thesis has been introduced the fundamental aspects of the thesis, including different resonant converter topologies, their modes of operation, control strategies and related applications.

The second part of the thesis is the central nucleus of this work, including chapters 2, 3, 4 and 5. In these chapters, the papers published in different journals and conferences are presented. In chapter 2 and 3, two different control strategies are proposed for a DC-DC CSPRC. The control strategy presented in chapter 4 is then developed to be applied to a multiple load DC-DC CSRC. Chapter 5 presents a robust control method for wireless energy transfer systems using current source resonant converter without any communication network.

Finally, the third part of the thesis is devoted to the analysis of the results obtained in the thesis (Chapter 6) and to the conclusions and future works derived from these works (Chapter 7). The chapter of analysis of the results tries to include the different strategies of control and to discuss critically the advantages, disadvantages and their fields of application.

1.9. PUBLICATIONS

[1] M. M. Ghahderijani, M. Castilla, A. Momeneh, J. T. Miret and L. G. de Vicuña, "Frequency-Modulation Control of a DC/DC Current-Source Parallel-Resonant Converter," in *IEEE Transactions on Industrial Electronics*, vol. 64, no. 7, pp. 5392-5402, July 2017.

[2] M. M. Ghahderijani, M. Castilla, A. Momeneh, J. T. Miret and L. G. de Vicuña, "Robust and Fast SlidingMode Control for a DC-DC Current-Source Parallel-Resonant Converter," *in IET Power Electronics*, in press.

[3] M. M. Ghahderijani, M. Castilla, J. Miret, R. Guzmán and J. M. Rey, "Control scheme for a multiple-output DC/DC current source parallel resonant converter," *2017 IEEE 26th International Symposium on Industrial Electronics (ISIE)*, Edinburgh, 2017, pp. 657-662.

[4] M. M. Ghahderijani, M. Castilla, Juan M. Rey, Javier Torres Martínez, and Miguel Andrés Garnica López, "A Communication-less Control Scheme for a Variable Air-gap Wireless Energy Transfer System using Current Source Resonant Converter," *IECON 2017 - 43nd Annual Conference of the IEEE Industrial Electronics Society*, China, 2017, in press.

[5] A. Momeneh, M. Castilla, M. Moradi Ghahderijani, J. Miret and L. García de Vicuña, "Analysis, design and implementation of a residential inductive contactless

energy transfer system with multiple mobile clamps," *in IET Power Electronics*, vol. 10, no. 8, pp. 875-883, 6 30 2017.

[6] A. Momeneh, M. Castilla, M. Moradi Ghahderijani, J. Miret and L. García de Vicuña, " Analysis, design and implementation of a DC/DC boost resonant-inductor converter with sliding-mode control," *in IET Power Electronics*, in press.

[7] Miret, Jaume; García de Vicuña, José L.; Guzmán, Ramón; Camacho, Antonio; Moradi Ghahderijani, Mohammad. 2017. "A Flexible Experimental Laboratory for Distributed Generation Networks Based on Power Inverters." *Energies* 10, no. 10: 1589.

[8] M. Castilla, A. Camacho, P. Marti, M. Velasco and M. Moradi Ghahderijani, "Impact of clock drifts on communication-free secondary control schemes for inverter-based Islanded Microgrids," in IEEE Transactions on Industrial Electronics, vol. PP, no. 99, pp. 1-1.

[9] A. Momeneh, M. Castilla, F. F. A. van der Pijl, M. Moradi and J. Torres, "New inductive contactless energy transfer system for residential distribution networks with multiple mobile loads," *2015 17th European Conference on Power Electronics and Applications (EPE'15 ECCE-Europe)*, Geneva, 2015, pp. 1-10.

[10] J. Torres-Martínez, M. Castilla, J. Miret, M. Moradi-Ghahderijani, J. Morales and R. Guzman, "Dynamic model of a grid-connected three-phase inverter with slope voltage control," *IECON 2015 - 41st Annual Conference of the IEEE Industrial Electronics Society*, Yokohama, 2015, pp. 001228-001233.

[11] M. M. Ghahderijani, M. Castilla, L. G. de Vicuña, A. Camacho and J. T. Martínez, "Voltage sag mitigation in a PV-based industrial microgrid during grid faults," *2017 IEEE 26th International Symposium on Industrial Electronics (ISIE)*, Edinburgh, 2017, pp. 186-191.

[12] M. M. Ghahderijani, M. Castilla, A. Momeneh, J. Morales and J. Miret, "Multi-objective optimized daily schedule for an efficient solar-based industrial microgrid," *IECON 2016 - 42nd Annual Conference of the IEEE Industrial Electronics Society*, Florence, 2016, pp. 3860-3865.

[13] A. Momeneh, M. Castilla, M. M. Ghahderijani, A. Camacho and L. G. de Vicuña, "Design and control of a small-scale industrial microgrid in islanding mode," *IECON 2016 - 42nd Annual Conference of the IEEE Industrial Electronics Society*, Florence, 2016, pp. 72-77.

[14] M. M. Ghahderijani, M. Castilla, A. Momeneh, R. G. Sola and L. G. de Vicuña, "Transient analysis of PV-based industrial microgrids between grid-connected and islanded modes," *IECON 2016 - 42nd Annual Conference of the IEEE Industrial Electronics Society*, Florence, 2016, pp. 365-370.

[15] Juan M. Rey, Javier Solano, Javier Torres Martínez, Jaume Miret, Mohammad Moradi Ghahderijani, Miguel Castilla, "Multi-layer active power and frequency control strategy for industrial microgrids," *IECON 2017 – 43rd Annual Conference of the IEEE Industrial Electronics Society*, China, 2017.

[16] Javier Torres Martínez, Miguel Castilla, Jaume Miret, Mohammad Moradi Ghahderijani, Juan M. Rey, "Experimental study of clock drift impact over droopfree distributed control for industrial microgrids," *IECON 2017 – 43rd Annual Conference of the IEEE Industrial Electronics Society*, China, 2017.

1.10. CONCLUSIONS

The state of the art related to resonant converters has been presented in this chapter including different resonant converter topologies, their modes of operation, control strategies and related applications. According to these studies, several unsolved problems have been mentioned. In fact, the main focus of this thesis is to find the best solutions for these problems. These solutions will be presented in detail in the next chapters.

CHAPTER 2

PUBLICATION I:
Frequency modulation control scheme for a DC/DC CSPRC

M. M. Ghahderijani, M. Castilla, A. Momeneh, J. T. Miret and L. G. de Vicuña, "Frequency-Modulation Control of a DC/DC Current-Source Parallel-Resonant Converter," in *IEEE Transactions on Industrial Electronics*, vol. 64, no. 7, pp. 5392-5402, July 2017.

Summary

CHAPTER 3

PUBLICATION II:

Robust and fast sliding-mode control for a DC-DC CSPRC

M. M. Ghahderijani, M. Castilla, A. Momeneh, J. T. Miret and L. G. de Vicuña, "Robust and Fast SlidingMode Control for a DC-DC Current-Source Parallel-Resonant Converter," *in IET Power Electronics*, in press.

ATTENTION ¡
Pages 40 to 50 of the thesis, containing the text mentioned above, should be consulted at the editor's web
https://ieeexplore.ieee.org/document/8281575/

Summary

CHAPTER 4

PUBLICATION III:

Control Scheme for a Multiple-Output DC/DC Current Source Parallel Resonant Converter

M. M. Ghahderijani, M. Castilla, J. Miret, R. Guzmán and J. M. Rey, "Control scheme for a multiple-output DC/DC current source parallel resonant converter," *2017 IEEE 26th International Symposium on Industrial Electronics (ISIE)*, Edinburgh, 2017, pp. 657-662.

Summary

CHAPTER 5

PUBLICATION IV:

A Communication-less Control Scheme for a Variable Air-gap Wireless Energy Transfer System using Current Source Resonant Converter

M. M. Ghahderijani, M. Castilla, Juan M. Rey, Javier Torres Martínez, and Miguel Andrés Garnica López, "A Communication-less Control Scheme for a Variable Air-gap Wireless Energy Transfer System using Current Source Resonant Converter," *IECON 2017 - 43nd Annual Conference of the IEEE Industrial Electronics Society*, China, 2017, in press.

ATTENTION ¡
Pages 60 to 66 of the thesis, containing the text mentioned above, are available at the editor's web
http://ieeexplore.ieee.org/document/8216090/

Summary

CHAPTER 6

Overview of the thesis and analysis of the results

Summary

This chapter analyzes the results obtained in the four publications in chapter 2 to 5. It presents the advantages and disadvantages of the proposed control schemes. New control solutions are also presented. These control solutions are the preliminary steps to reach the final solutions presented in publications 1 and 2. In addition, new relevant results that were already obtained but were not included in the publications due to space limitations, are included to complement this chapter.

6.1. INTRODUCTION

In this chapter, some preliminary control solutions are presented for the publications I and II. It is worth mentioning that these solutions were the first control methods studied in this thesis. These solutions were necessary in order to reach the final control solutions presented in the publications I and II. For instance, a preliminary non-linear control solution is presented for frequency-modulation control scheme. Afterward, the non-linear control was replaced by the cascaded two-loop control system presented in Chapter 2.

Furthermore, some other preliminary sliding surfaces are presented for sliding mode control presented in chapter 3. These surfaces are based on the second method of Lyapunov. In addition, the Class-D CSPRC is developed in this chapter by adding a new switch between diode bridge rectifier and the output load. Afterward different sliding mode control schemes with two configurations based on Lyapunov and linear sliding curves are presented for this topology. As stated, all these control methods were the initial attempts to achieve the control solution in publication II. So as will be explained in section 6.3, among all these control solutions, the final control solution presented in chapter 3 is selected for the publication.

This chapter also conducts a comparison among the final proposed control methods for Class-D CSPRC presented in the publications I and II. This comparison will be performed in two cases of static and dynamic analysis. The other analysis will be performed on the impacts of the sliding mode control in other applications of current source resonant converter, i.e., multiple-output power switching supply (Chapter 4) and wireless power transfer system (Chapter 5).

Finally, new relevant simulation results that were already obtained but were not included in the publications due to space limitations, are included to complement this chapter.

6.2. FREQUENCY MODULATION CONTROL SYSTEMS (PUBLICATION I)

In this section, different aspects of the publication presented in chapter 2 are developed. In addition, a non-linear control structure is presented for the Class-D CSPRC. Then a brief comparison is presented to highlight the benefits and drawbacks of the control solutions based on the frequency modulation control system.

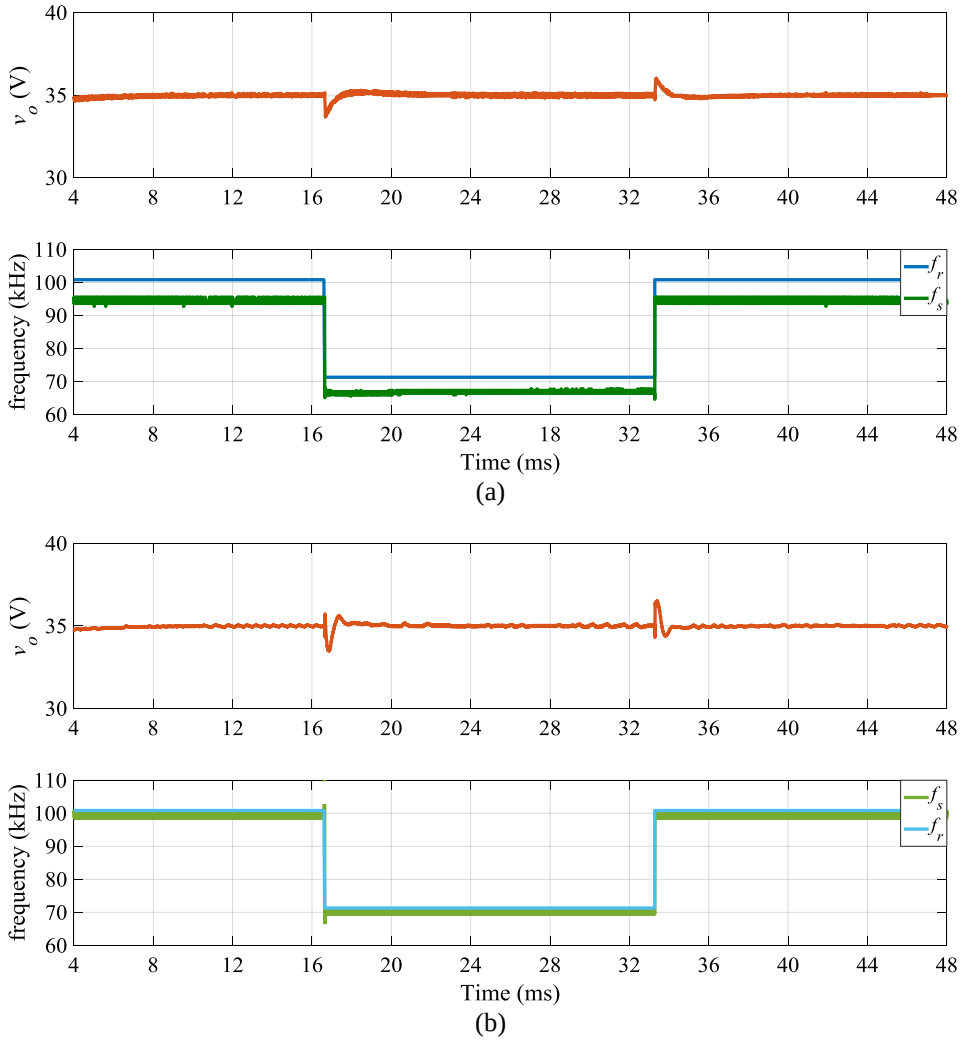

Fig. 6.1. Transient response of the converter against resonant inductor step changes from 5.3µH to 10.6 µH for: a) full-load condition, b) 10% of the full-load condition

6.2.1 EXTENSION OF THE SIMULATION RESULTS

In this section, some results of the Chapter 2, which were not included in the paper due to the lack of space are included. For instance, to have a clear understanding about the robustness of the proposed control solution, this section is extended. In the publication I, the transient response against load step changes has been presented for different values of the input voltage. However, the robustness against variations in some variables such as resonant components, the output voltage reference and the input voltage were not presented. So, in this subsection, some new results are presented to cover this issue. Fig. 6.1 shows the transient response of the proposed control scheme against step variations in the resonant inductor. Although this type of changes is not usual in practice, the idea here is to evaluate this extreme disturbance. Even in this case, the output voltage is perfectly regulated and the

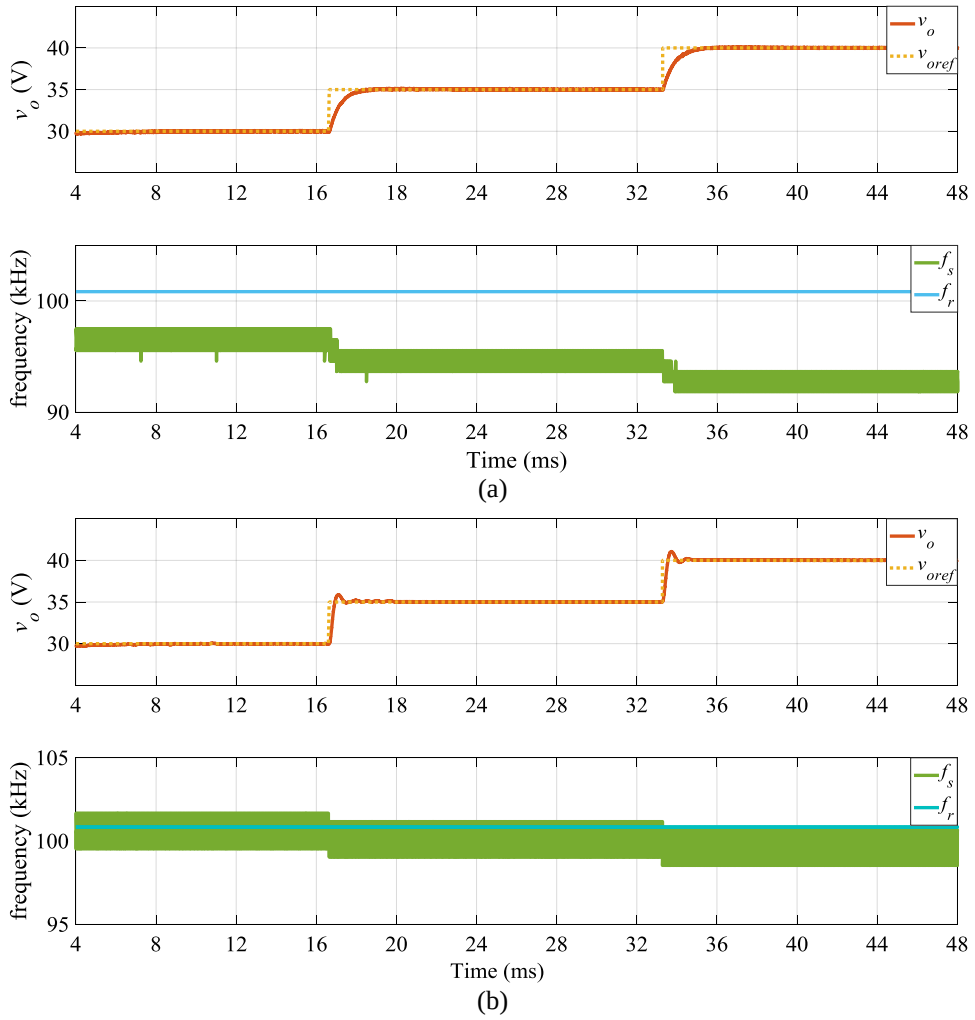

Fig. 6.2. Transient response of the converter against output voltage reference changes for: a) full-load condition, b) 10% of the full-load condition

swiching frequency is lower but close to the resonant freuqncy, as expected by the theoretical analysis in chapter 2.

Fig. 6.2 shows the transient response against the changes in the output voltage reference. As can be seen, the output voltage reference is perfectly tracked by changing the switching frequency based on the curves plotted in Fig. 2 in Chapter 2.

Finally, input voltage step changes are applied to the converter. As shown in Fig. 6.3, the robustness of the control solution in this case is also proved.

6.2.2. PRELIMINARY CONTROL SOLUTION

6.2.2.1. Synthesis of the non-linear control system

In this subsection, a non-linear frequency modulation control structure is proposed for the Class-D current source resonant converter. The proposed control scheme is shown in Fig. 6.4.

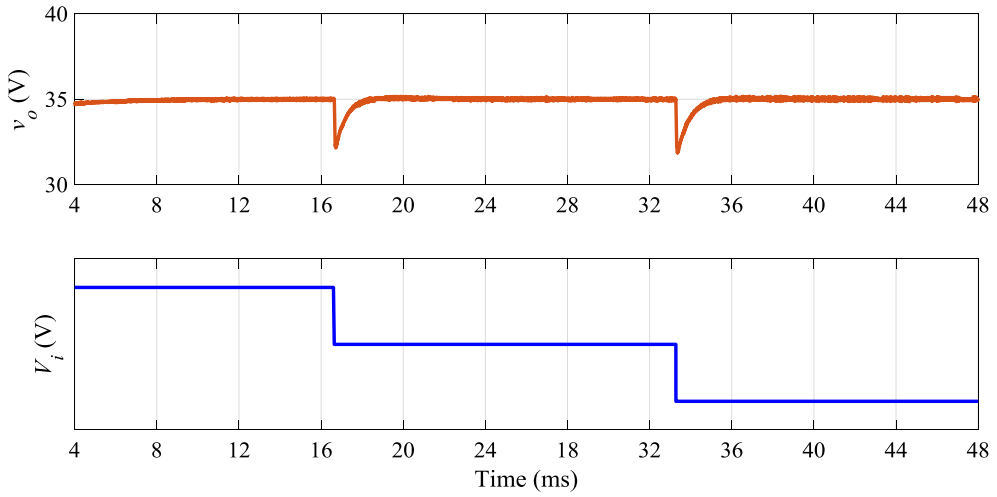

Fig. 6.3. Transient response of the converter against input voltage step changes in full load condition

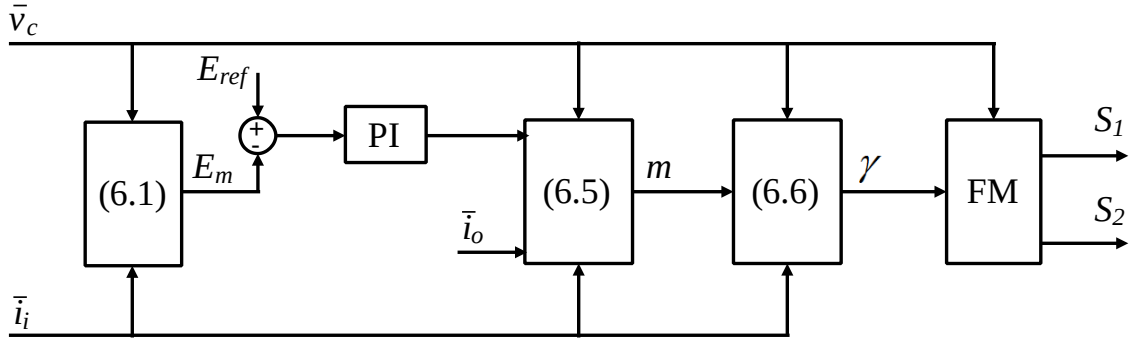

Fig. 6.4. Proposed non-linear control scheme

The first step is to obtain the energy function. So, applying the method presented in [70] to the Class-D current source resonant converter, the measured and reference energy functions are obtained:

$$E_m = \frac{1}{2} C_{eq} \bar{v}_c^2 + \frac{1}{2} L_i \bar{i}_i^2 \tag{6.1a}$$

$$E_{ref} = \frac{1}{2} C_{eq} V_{cref}^2 + \frac{1}{2} L_i \frac{V_{cref}^2}{R V_i} \tag{6.1b}$$

To eliminate the energy error, this signal is then passed through a PI controller.

The next step is to find an adequate equation for signal *m*. Note that as stated in Chapter 2, *m* is a variable that contains information about the system state in an averaged sense (through the $\bar{v}_c$ and $\bar{i}_i$) and the control action ω_s. Taking into consideration an ideal switching converter, the following expression is obtained by assuming zero power losses:

$$V_i \bar{i}_i = \frac{n_s}{n_p} \bar{v}_c \bar{i}_o \tag{6.2}$$

Differentiating the above equation along the variables, we obtain:

$$V_i \frac{d\bar{i}_i}{dt} = \frac{n_s}{n_p} \left(\bar{v}_c \frac{d\bar{i}_o}{dt} + \bar{i}_o \frac{d\bar{v}_c}{dt} \right) \tag{6.3}$$

Applying the energy compensation into account, a new term is added to (6.3) as below:

$$V_i \frac{d\bar{i}_i}{dt} - \mathrm{PI}(E_{ref} - E_m) = \frac{n_s}{n_p} \left(\bar{v}_c \frac{d\bar{i}_o}{dt} + \bar{i}_o \frac{d\bar{v}_c}{dt} \right) \tag{6.4}$$

So, inserting the averaged model equations obtained in chapter 2 in (6.4), the variable *m* is achieved as below:

$$m = \frac{\frac{V_i^2}{L_i} + \left(\frac{n_s}{n_p}\right)^2 \frac{\bar{i}_o^{\,2}}{C_{eq}} - \frac{n_s}{n_p} \left(\bar{v}_c \frac{d\bar{i}_o}{dt} \right) - \mathrm{PI}(E_{ref} - E_m)}{\frac{n_s}{n_p} \left(\frac{\bar{v}_c V_i}{L_i} + \frac{\bar{i}_o \bar{i}_i}{C_{eq}} \right)} \tag{6.5}$$

The variable *m* is then used for obtaining the input signal of the modulator (γ) based on the equation (10) in chapter 2 :

$$\gamma = \frac{\omega_s}{\omega_r} = \frac{A + \sqrt{A^2 + 4}}{2} \tag{6.6}$$

where A is defined as below:

$$A = \frac{\omega_s}{\omega_r} - \frac{\omega_r}{\omega_s} = \frac{-4Z_0}{\pi^2} \frac{\bar{i}_i}{\bar{v}_c} \sqrt{1 - m^2} \tag{6.7}$$

6.2.2.2. Simulation results

The objective of this subsection is to verify, by simulation, the validity of the proposed non-linear controller with the system parameter values listed in Table 6.1.

Fig. 6.5. shows the start-up results of the resonant voltage for different reference voltage values V_{cref}. As can be seen, there is a steady state error in the voltage.

TABLE 6.1. VALUES OF THE POWER COMPONENTS

Symbol	Quantity	Value
V_i	Input voltage	12 V
L_i	Input filter inductor	300 µH
C_r	Resonant capacitor	470 nF
L_r	Resonant inductor	5.3 µH
n_p:n_s	Transformer turns ratio	1:1
L_o	Output filter inductor	100 µH
C_o	Output filter capacitor	470 µF
R	Full-load resistor	20 Ω

6.2.2.3. Comparison with the control solution in publication I

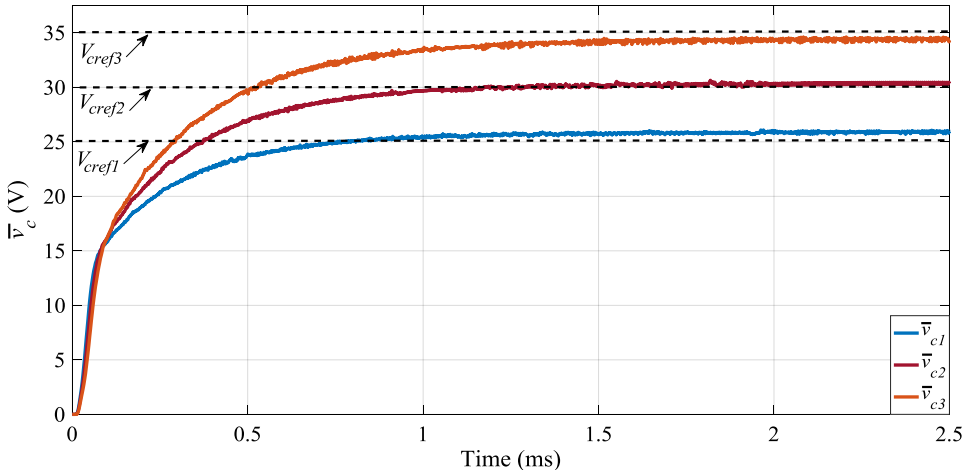

Fig. 6.5. Startup simulation of the resonant capacitor voltage

To sum up, the practical use of this non-linear controller is limited due to some drawbacks: complexity of implementation of the control and appearance of an error in the output voltage in steady state. These problems are then solved in the control solution presented in publication I by proposing a cascaded two-loop control scheme.

6.3. SLIDING MODE CONTROL SYSTEM (PUBLICATION II)

In this section, various sliding surfaces are analyzed to be applied first to the Class-D CSPRC and then to an alternative developed topology. The alternative topology is composed of an additional switch between the diode rectifier and the load. In this case, an additional control input is required. This issue is discussed later in the next subsections.

6.3.1 EXTENSION OF THE SIMULATION RESULTS

In this section, some results of the Chapter 3, which were not included in the Publication II are presented. These results are presented to prove the robustness of the proposed control solution.

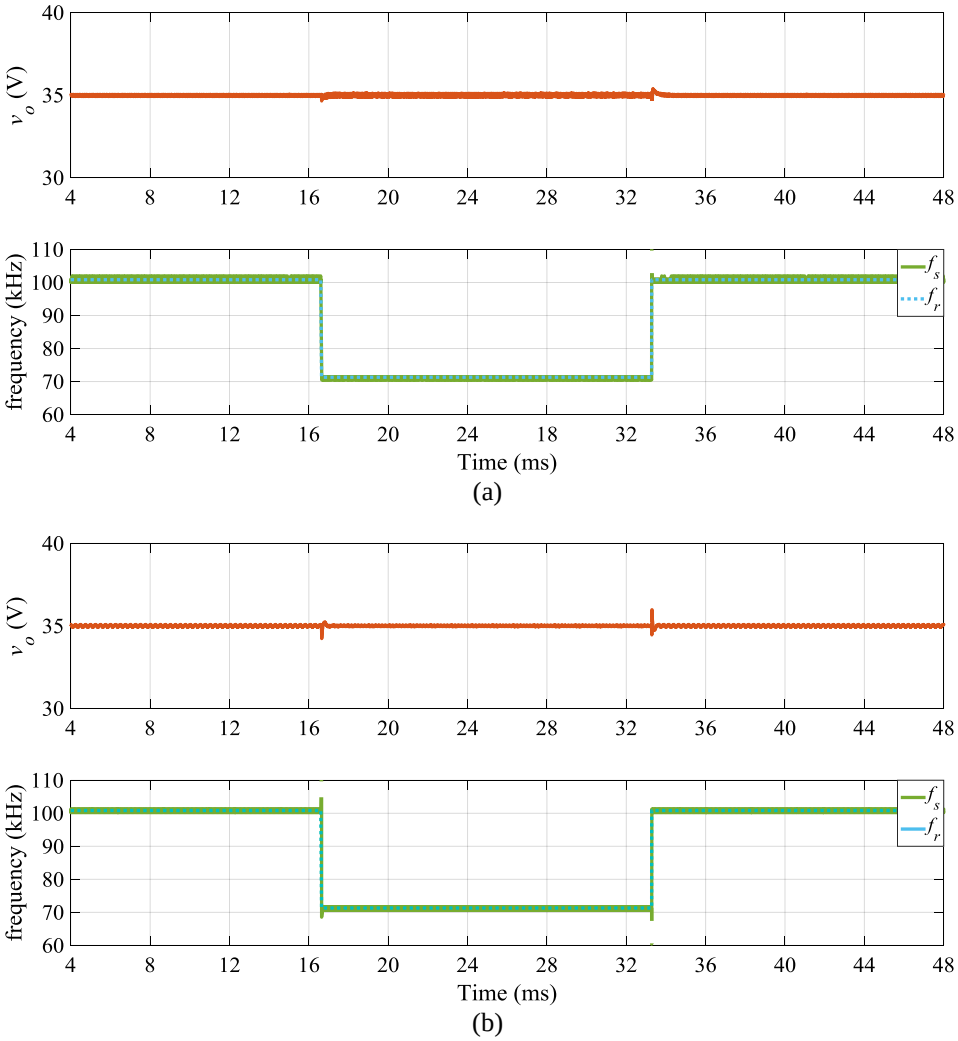

Fig. 6.6. Transient response of the converter against resonant inductor step changes from 5.3µH to 10.6 µH for: a) full-load condition, b) 10% of the full-load condition

Fig. 6.6 shows the excellent transient response of the proposed control scheme against the variation in the resonant inductor. In this case, the output voltage is regulated fast and the resonant frequency is tracked by the switching frequency, as expected by the theoretical analysis in chapter 3.

Fig. 6.7 shows the transient response against the changes in the output voltage reference. As can be seen, both the output voltage reference and resonant frequency are perfectly tracked.

Finally, an input voltage step change is applied to the converter. As shown in Fig. 6.8, both the fast transient response and the robustness of the control solution in this case is also proved.

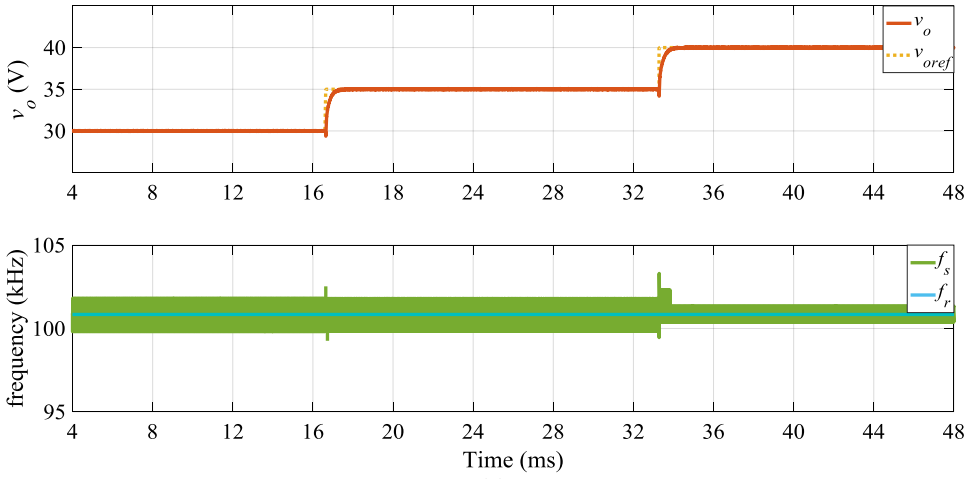

(a)

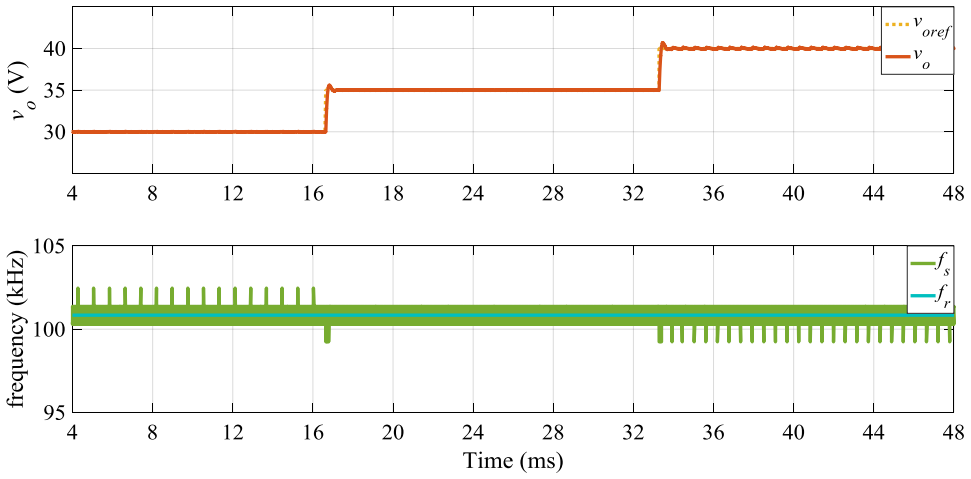

(b)

Fig. 6.7. Transient response of the converter against output voltage reference changes for: a) full-load condition, b) 10% of the full-load condition

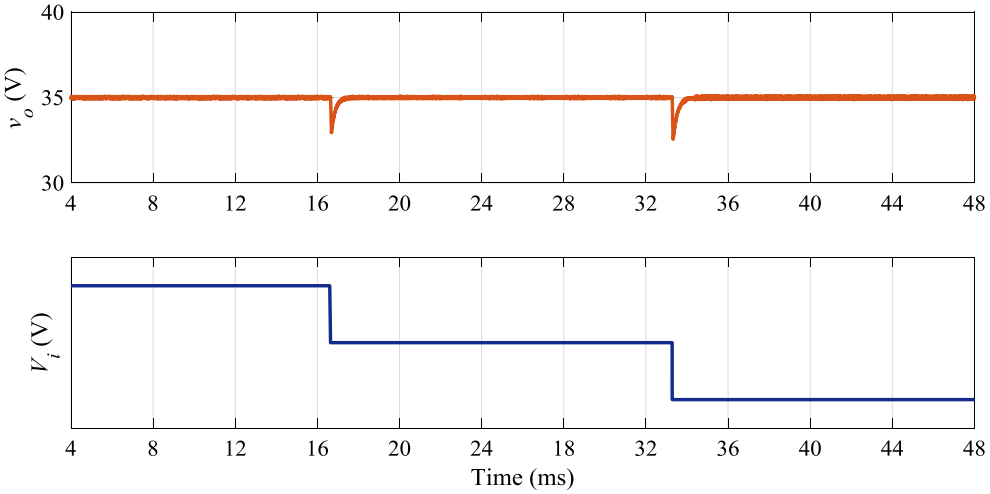

Fig. 6.8. Transient response of the converter against input voltage step changes in full load condition

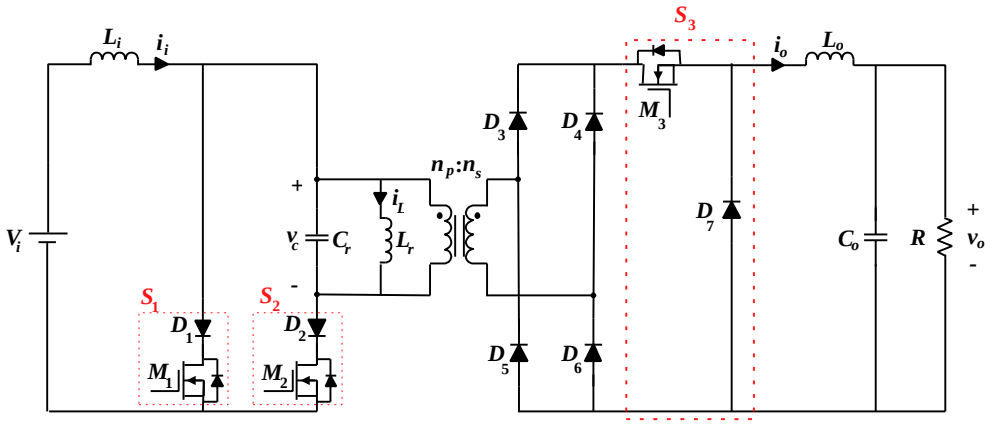

Fig. 6.9. Class-D CSPRC with an additional switch

6.3.2. PRELIMINARY CONTROL SOLUTIONS

In this section, various preliminary sliding surfaces are presented for the sliding mode control scheme for the Class-D CSPRC in chapter 3. These surfaces are based on the second method of Lyapunov. In addition, another alternative is proposed in this section by developing the Class-D CSPRC shown in Fig. 6.9 by adding a new switch between the diode bridge rectifier and the output load. Afterward different sliding surfaces are tested for this topology including the Lyapunov and linear sliding curves. As mentioned, all these control solutions were the initial attempts to achieve the control solution in publication II. Hence, at the end of this section, a brief comparison with the control solution in publication II is presented to show the superiority of the control solution in chapter 3.

6.3.2.1. Alternative Class-D CSPRC topology with two control actions

The converter shown in chapter 3 has a unique control action, associated with the energy transfer between the input source and the resonant tank. Adding a new switch as shown in Fig. 6.9 provides greater flexibility to the converter, since it allows to separate the energy transfer between the tank and the load from the operating mode selected for the output converter switches. In particular, the resonant tank transfers energy to the load when the switch S_3 is in conduction, otherwise, the power supply to the load is interrupted.

However, this topology increases the complexity of the control and reduces the total efficiency of the system, as will be shown in the next subsections.

6.3.2.2 Basic Lyapunov-based sliding mode control system

The Lyapunov-based systematic approach presented in [70] is developed for the sliding mode control design of the Class-D CSPRC.

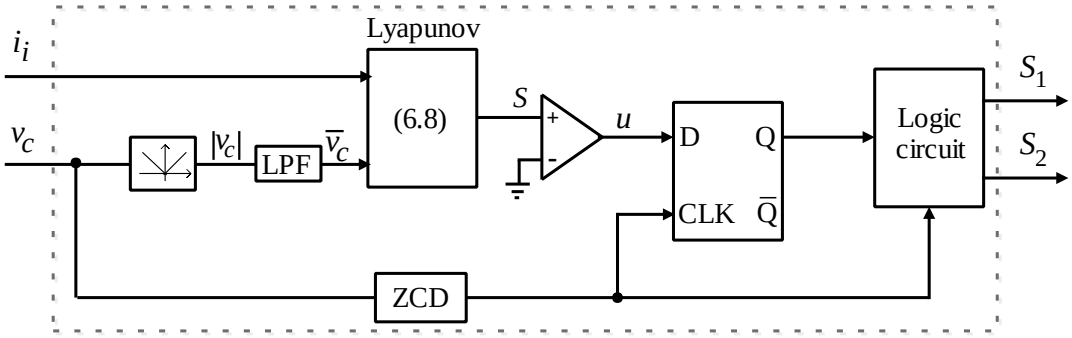

Fig. 6.10. Proposed Lyapunov based sliding mode control scheme with only one control action

A. Class-D CSPRC with one control action

By applying the method presented in [70], Lyapunov sliding surface for Class-D CSPRC with one control action and its associated control law result in:

$$S = \frac{\mathrm{V}_{oref}}{R\mathrm{V}_i}\bar{v}_c - \bar{i}_i \tag{6.8}$$

$$u = \begin{cases} 1 & S > 0 \\ 0 & S < 0 \end{cases} \tag{6.9}$$

Fig. 6.10 shows the Lapunov based sliding mode control scheme proposed for the Class-D CSPRC with one control action. In general, the control system is composed of a sensing circuitry, a stage for generating the sliding surface, the control law, and a switching logic block. In this control scheme, the regulation is based on only two measurements of input current and resonant voltage. These measurements are used to obtain the sliding surface based on the second method of Lyapunov designed as (6. 8). Afterward, the control signal *u* is assigned based on the control law defined in (6.9). This control signal is then applied to the amplitude modulator to generate the switching gate signals for the Class-D resonant inverter.

B. Class-D CSPRC with two control actions

Using the same methodology, the sliding surfaces and the design conditions for the converter with two control actions are obtained as below:

$$S_1 = \frac{\mathrm{V}_{oref}^2}{R\mathrm{V}_i\mathrm{V}_{cref}}\bar{v}_c - \bar{i}_i \qquad S_2 = \frac{\mathrm{V}_{oref}}{R\mathrm{V}_{cref}}\bar{v}_c - \bar{i}_o \tag{6.10}$$

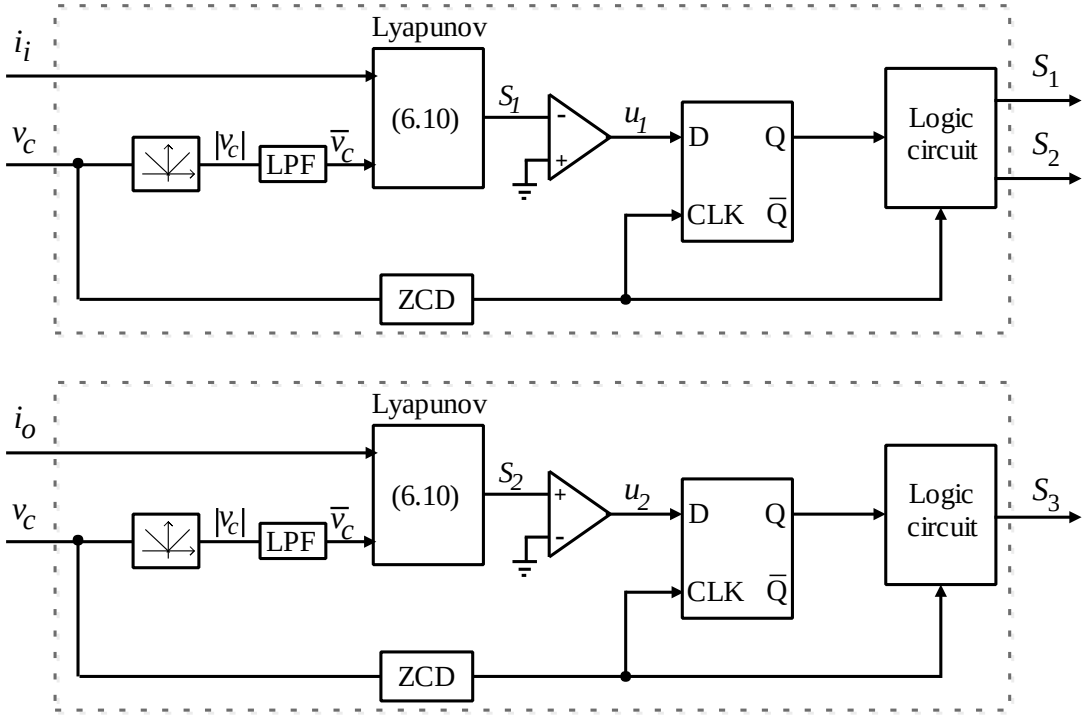

Fig. 6.11. Proposed Lyapunov based sliding mode control scheme with two control actions

$$u_1 = \begin{cases} 0 & S_1 > 0 \\ 1 & S_1 < 0 \end{cases} \qquad u_2 = \begin{cases} 1 & S_2 > 0 \\ 0 & S_2 < 0 \end{cases} \tag{6.11}$$

$$\mathrm{V}_{cref} > \mathrm{V}_i \qquad 0 < \mathrm{V}_{oref} < \mathrm{V}_{cref} \tag{6.12}$$

Fig. 6.11 shows the complete control structure for this case. Note that the state change of the new switch S3 is only occurred at the zero crossings of the resonant voltage, which guarantees zero switching losses in this switch, as well.

C. Simulation results

Fig. 6.12 and Fig. 6.13 shows transient responses using the proposed Lyapunov's sliding mode control scheme for the Class-D CSPRC with one and two control actions, respectively. Note that the output voltage presents a load-dependent steady-state error, thereby causing a poor regulation of the output voltage.

6.3.2.3. Lyapunov-based sliding mode control with integral terms

The theoretical studies carried out in previous subsection have not foreseen the appearance of an error in the output voltage in steady state. The steady state error can be observed clearly in the simulations. The existence of the error is basically due to the imperfections and delays that take place in the control loops.

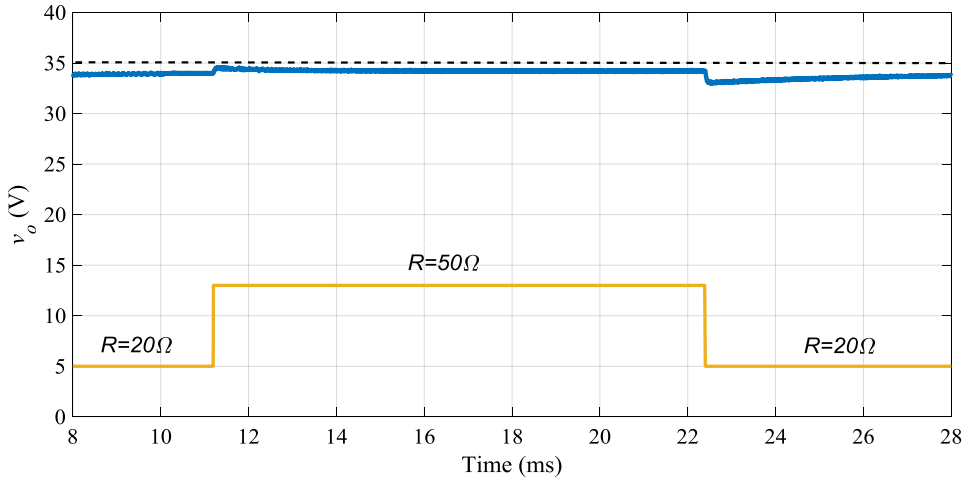

Fig. 6.11. Load step change transient response and steady-state result of the output voltage in a Class-D CSPRC with one control action based on the presented Lyapunov-based control scheme.

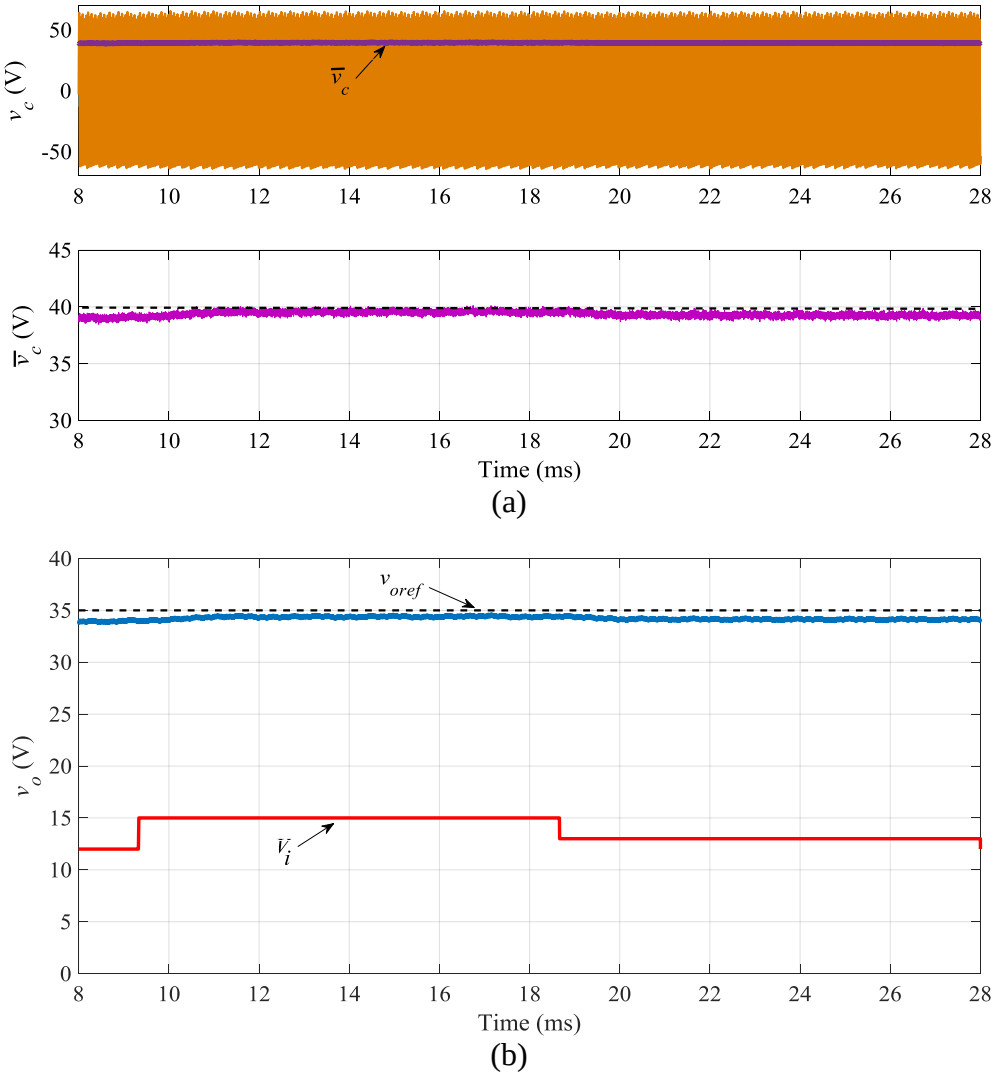

Fig. 6.12. Input voltage step change transient response and steady-state results of a Class-D CSPRC with two control actions based on the presented Lyapunov-based control scheme: (a) resonant capacitor voltage (b) output voltage

A possible solution to eliminate this error is to include an integral term in the sliding

surface. This term memorizes the error that is being committed, in order to counteract it until it is being canceled. Hence, in this subsection a new sliding surface is presented to ensure the correct operation of the regulators without the presence of these errors.

A. Class-D CSPRC with one control action

One of the additional advantages of the use of integral terms in the sliding surfaces is their dynamic nature so that the principle of operation of the integrators makes them to be adapted to each new situation taking at all times the necessary value to compensate the error in the output voltage.

The new sliding surface containing integral term can be written as below:

$$S = \frac{\mathrm{V}_{oref}}{R\mathrm{V}_i}\bar{v}_c + k_i \int (v_{oref} - \bar{v}_o)dt - \bar{i}_i \tag{6.13}$$

$$u = \begin{cases} 1 & S_2 > 0 \\ 0 & S_2 < 0 \end{cases} \tag{6.14}$$

The first term $\frac{\mathrm{V}_{oref}}{R\mathrm{V}_i}\bar{v}_c$ is a feed-forward term that accelerates the converter dynamics while the integral term is in charge of eliminating the caused error.

B. Class-D CSPRC with two control actions

For the converters governed by two control inputs, the integrator is only added to the switching surface that regulates the output voltage. So, the sliding surfaces are

$$S_1 = \frac{\mathrm{V}_{oref}^2}{R\mathrm{V}_i\mathrm{V}_{cref}}\bar{v}_c - \bar{i}_i \qquad S_2 = \frac{\mathrm{V}_{oref}}{R\mathrm{V}_{cref}}\bar{v}_c + k_i \int (v_{oref} - \bar{v}_o)dt - \bar{i}_o \tag{6.15}$$

$$u_1 = \begin{cases} 0 & S_1 > 0 \\ 1 & S_1 < 0 \end{cases} \qquad u_2 = \begin{cases} 1 & S_2 > 0 \\ 0 & S_2 < 0 \end{cases} \tag{6.16}$$

However, the utilization of such surfaces is strongly limited by some practical drawbacks. The problem is the complexity of the hardware required to implement these nonlinear functions, which usually depend on the input voltage, the load, and a considerable number of state variables. This is a general limitation shared by other Lyapunov based control schemes (in fact, the problem is in the feed-forward terms, not in the integral terms).

6.3.2.4. Equivalent control-based sliding mode control system

In this subsection, an alternative approach for the synthesis of sliding surfaces is proposed. The focus will be on the use of linear stabilizing terms as a way of generating

easy-to implement control circuits. First, the sliding surface for the single-input converter is presented and next the case of multi-input converter is introduced. Then a comparison is done by providing some simulation results.

A. Class-D CSPRC with one control action

This case was already developed in Chapter 3 by first introducing a theoretical analysis on dynamic modeling and then by proposing a sliding mode control scheme with following sliding surface:

$$S = k_p(v_{oref} - \bar{v}_o) + k_i \int (v_{oref} - \bar{v}_o)dt - \bar{i}_i \tag{6.17}$$

$$u = \begin{cases} 1 & S_2 > 0 \\ 0 & S_2 < 0 \end{cases} \tag{6.18}$$

In addition, a design procedure for determining the values of the control parameters was presented. The theoretical contributions were experimentally validated by selected tests on a laboratory prototype.

B. Class-D CSPRC with two control actions

This section is dedicated to the control system of a Class-D CSPRC with two control actions. The sliding surfaces are defined as below:

$$\begin{aligned} S_1 &= k_{p1}\left(v_{cref} - \bar{v}_c\right) + k_{i1} \int (v_{cref} - \bar{v}_c)dt - \bar{i}_i \\ S_2 &= k_{p2}\left(v_{oref} - \bar{v}_o\right) + k_{i2} \int \left(v_{oref} - \bar{v}_o\right)dt + k_{d2} \frac{d}{dt}\left(v_{oref} - \bar{v}_o\right) \end{aligned} \tag{6.19}$$

$$u_1 = \begin{cases} 0 & S_1 > 0 \\ 1 & S_1 < 0 \end{cases} \qquad u_2 = \begin{cases} 1 & S_2 > 0 \\ 0 & S_2 < 0 \end{cases} \tag{6.20}$$

Fig. 6.13 shows the control scheme of the Class-D CSPRC with two control actions based on the linear sliding surfaces (6.19).

C. Simulation results

The simulation results of the Class-D CSPRC are shown in this subsection. The common power-circuit parameters used in all simulations are the values listed in Table 6.1. Fig. 6.14 shows the effect of integral term on the steady-state error of the output voltage by considering a fixed proportional term. Note that in both cases, a similar dynamic is obtained, but the presence of the integrator eliminates the output voltage steady-state error.

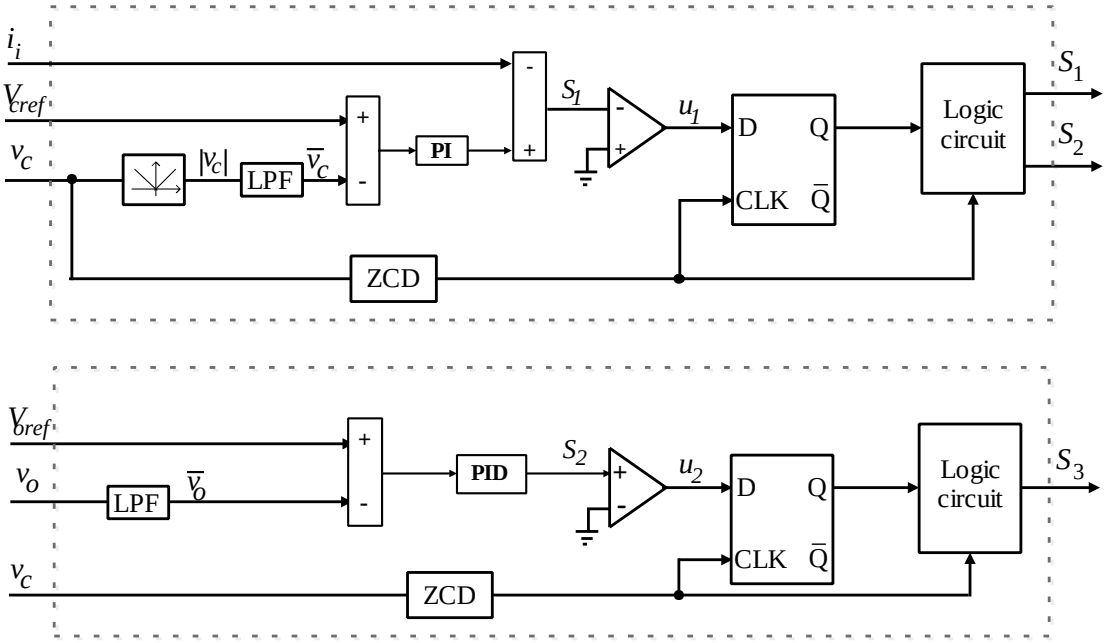

Fig. 6.13. Proposed control scheme for the Class-D CSPRC with two control actions based on the linear sliding surfaces

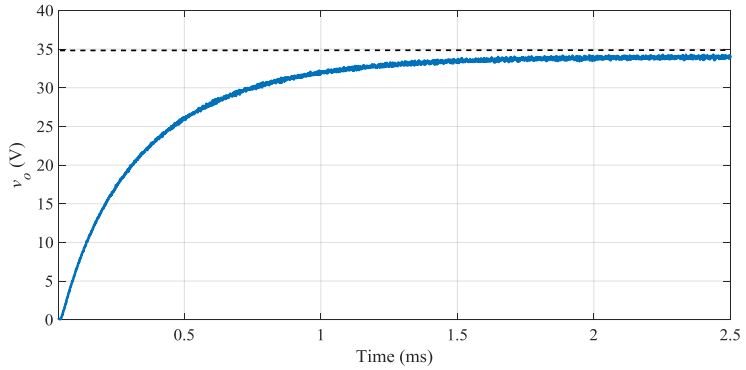

(a)

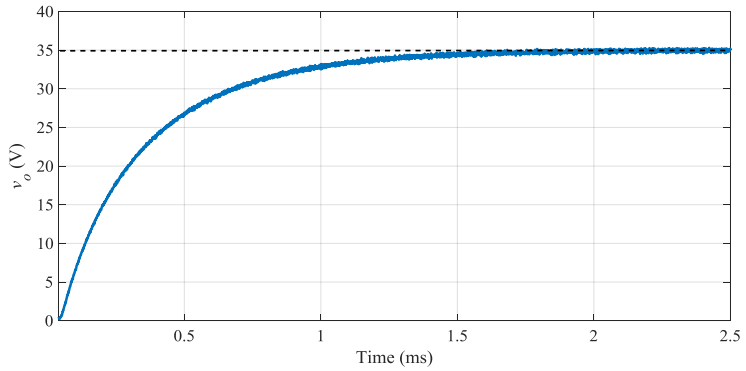

(b)

Fig. 6.14. Proposed control scheme for the Class-D CSPRC with two control actions based on the linear sliding surfaces: (a) without the integral term in S_2 and (b) with the integral term in S_2

Figs. 6.15 and 6.16 compare simulation results of the Class-D CSPRC with one and two control actions using the linear sliding curves. Excellent agreement is obtained for steady state and large-signal transient responses against load step changes from full-load to 10% of

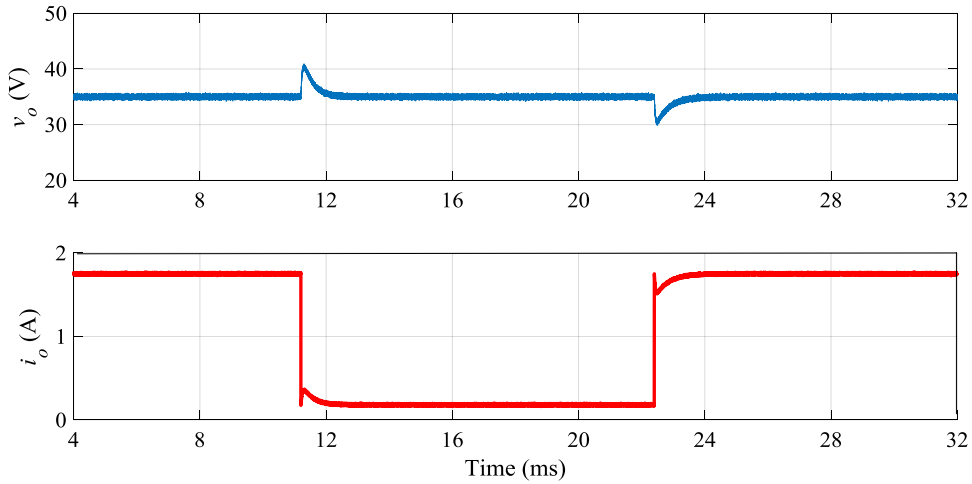

Fig. 6.15 Transient response of the Class-D CSPRC with one control action based on the linear sliding surfaces

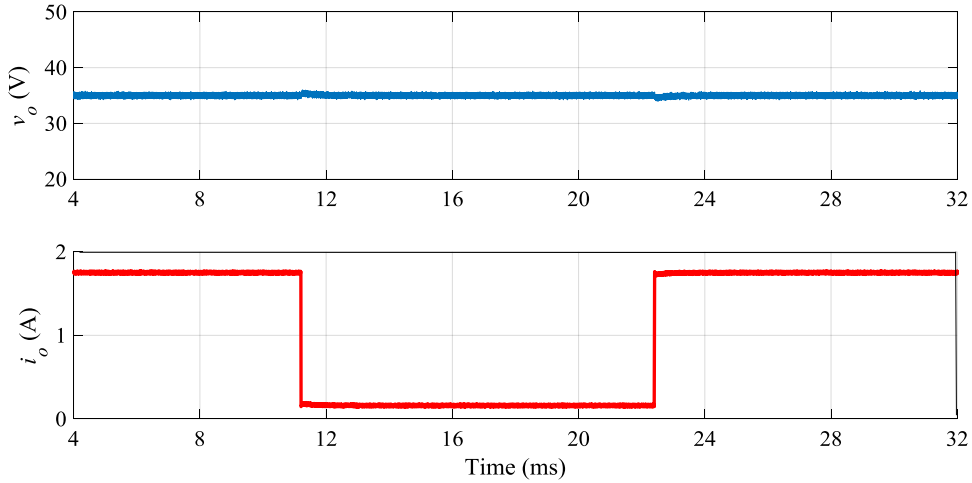

Fig. 6.16. Transient response of the Class-D CSPRC with two control actions based on the linear sliding surfaces

the full-load condition and vice-versa. Moreover, good output performances (such as nonzero steady-state errors, stable operation, low steady-state ripple, fast transient responses, and high robustness) are obtained in relation to results obtained for Lyapunov-based control systems.

6.3.2.5. Comparison with the control solution in publication II

To sum up, compared to the enhanced control scheme is Publication II, for the case with two control actions, the same transient response is obtained. However, in this case there are five control parameters, i.e., k_{p1}, k_{i1}, k_{p2}, k_{i2} ,and k_{d2} . Hence, a more complex control design is necessary. In addition, the efficiency is lower, because there are two elements more in power circuit (S_3 and D_7).

Table. 6.2. General comparison with the state of the art

Ref.	objectives			robustness against parameter variation
	ZVS	resonant frequency tracking	output voltage regulation	
[33], 2006	✓	✓	×	×
[71], 2010	✓	✓	×	×
[36], 2014	✓	✓	×	×
[34], 2012	✓	✓	×	×
[35], 2012	✓	✓	×	×
[72], 1997	✓	✓	✓	×
[37], 2010	✓	✓	✓	×
[73], 2014	✓	✓	×	✓
Proposal Pub. I	✓	×	✓	✓
Proposal Pub. II	✓	✓	✓	✓

6.4. COMPARISON AND ANALYSIS OF THE RESULTS IN PUBLICATIONS I AND II

In this section, at first, a comprehensive comparison between the state-of-the-art and the proposals is presented in table 6.2. As shown in the table, the presented control schemes combine some interesting objectives: output voltage regulation, ZVS and the resonant frequency tracking. Furthermore, the proposals are robust against the variation in system parameters. In contrast, some of state-of-the-art schemes reach similar objectives but independently, without combining them in a single scheme.

Then, a general comparison is performed between the proposed control schemes in Publications I and II as stated in Table 6.3.

The modulation technique used in the first publication is a frequency modulation technique. Hence, the control signal is the switching frequency of the resonant inverter (f_s). The idea is to change the switching frequency, but just below resonant, so close to resonant frequency to achieve the control objectives defined in previous sections. Furthermore, to model the system, harmonic linearization and harmonic balance method is used. For control design, the closed-loop transfer functions of the system are first obtained by using the

Table. 6.3. General comparison between proposed control methods

	Modulation	Control signal	Modeling method	Control design	N of measurements
Publication I	Frequency	f_s	Harmonic linearization & Harmonic balance	Frequency-domain method	Basic Scheme: 3 Enhanced Scheme:4
Publication II	Amplitude	u	Harmonic linearization & Harmonic balance	Time-domain method	Basic Scheme: 3 Enhanced Scheme:4

derived small-signal model. Afterward, the frequency-domain specifications of the closed-loop system are fixed in terms of desired control bandwidth and phase margin. Finally, bode diagrams of different set of gain values are examined until the specifications are met. The gain values of the PI controllers satisfying the specifications are selected.

In the second publication, i.e., the sliding mode control scheme, the control signal is the discrete parameter u. Actually this control scheme is based on amplitude modulation technique. So, signal u determines the operation mode of the converter, i.e., energizing or de-energizing modes to change the amplitude of the resonant voltage. The idea is to switch between these two modes, to satisfy the defined control objectives. In this publication, as in previous case, harmonic linearization and harmonic balance methods are applied to obtain the large signal average model of the system. In addition, to design the proposed robust control, closed-loop dynamics of the system is first obtained based on the equivalent control theory. This model is then linearized around its equilibrium point to be used in the stability analysis.

Note that, in both proposed control schemes, three variables of input current, resonant capacitor voltage and output voltage are measured and send to the control platform. Moreover, for the enhanced control schemes, to have a fast transient response, an additional measurement, i.e., output current is also necessary.

The next comparison is done in terms of static and dynamic analysis. The static term includes the analysis about steady state output voltage tolerance, range of switching frequency, variation of resonant voltage, and efficiency. The dynamic properties that are included in the analysis are transient response time, voltage deviation and robustness against some external disturbances. It is worth mentioning that the values of the input and output

Table. 6.4. Static result comparison between proposed control methods

Publication	Δv_o (V)	f_{smin} (kHz)	f_{smax} (kHz)	v_c (V)				η (%)	ZVS
				up		down			
				max	min	max	min		
Pub. I	0	94	100	60	60	-60	-60	94	√
Pub. II	0	100.8	100.8	75	50	-50	-75	98	√

voltages and the components of the CSPRC are maintained fixed during the comparison. These values are listed in table 6.1.

6.4.1. Static analysis

Table 6.4 lists the static results obtained by the proposed control schemes. As can be seen, both control schemes provide a perfect output voltage regulation, so that there is no error in the output voltage in steady-state condition ($\Delta v_o = v_o - v_{oref} = 0$). Furthermore, ZVS condition is guaranteed in both presented control schemes.

The control scheme presented in publication I is based on the frequency modulation technique so the control signal is the switching frequency of the resonant inverter. So, by applying a load variation, the switching frequency f_s changes in order to regulate the output voltage. The switching frequency varies between 94 to 100 kHz for full-load and 10% of full-load condition, respectively. Although the switching frequency is below resonance, it is so close to the resonant frequency, ensuring a good regulation without reducing the efficiency.

Publication II uses an amplitude modulation technique. So the influenced parameter is the amplitude of the resonant capacitor voltage. As can be seen, the amplitude of the resonant voltage in publication I is somehow constant. While, in publication II, the resonant capacitor voltage is varying depending on the value of the control signal u. In this case the variation range of v_c is approximately 25 V.

Finally, taking efficiency into account, SMC has better response. For example, in full-load condition, SMC gives an efficiency of about 4% more than frequency modulation control. In fact, the conduction losses are nearly the same for both control schemes.

Table. 6.5. Static result comparison between converter switching frequency

Variable	Value	f_r (kHz)	Pub. I		Pub. II	
			f_s (kHz)		f_s (kHz)	
			FL	10% FL	FL	10% FL
L_r (µH)	5.3	100.8	94	100	100.8	100.8
	10.6	71	67	70	71	71
V_{ref} (V)	30	100.8	96	100	100.8	100.8
	35	100.8	94	100	100.8	100.8
	40	100.8	92	100	100.8	100.8

However, the switching losses are lower with amplitude modulation than with frequency modulation. The reason is that the converter operates exactly at resonant frequency for all the load range with amplitude modulation while the switching frequency is slightly lower than the resonant frequency with frequency modulation. This issue is clearly shown in Table 6.5 which is the summary of the Fig. 6.6 and Fig. 6.7.

6.4.2. Dynamic analysis

Table 6.6 presents the obtained results of some dynamic properties of the proposed control schemes such as transient response time T_r, voltage deviation VDF, and some robustness factors.

The results show that SMC control provides slightly better transient response and voltage deviation. However, both control methods are robust against parameter variations. Actually both controls show a robust behavior against any parameter variations such as step changes in input voltage, output reference voltage and even in resonant circuit parameters.

So, it can be concluded that, in majority of the cases, both control schemes ensure all the control objectives. So it is not easy to state which one is the best.

Actually, both have some benefits and drawbacks. For example, in SMC control scheme, the resonant voltage is suffering from a variation in amplitude in steady-state which may limit its practical use in some applications.

In contrary, in frequency modulation control, although the resonant capacitor voltage amplitude is constant in steady-state, the transient response is not much good as the SMC control.

Therefore, depending on the application, one of these two control scheme can be used.

Table. 6.6. Dynamic result comparison between proposed control methods

Publication			Pub. I	Pub. II
Step change R_o	T_r (ms)	Basic control $K_o = 0$	1.8	1.6
		Enhanced control $K_o = 2.9$	0.4	0.3
	VDF (%)	Basic control $K_o = 0$	2	1.7
		Enhanced control $K_o = 2.9$	0.7	0.5
Step change L_r	T_r (ms)	FL	2	0.5
		10% of FL	2.1	0.7
	VDF (%)	FL	4	2
		10% of FL	5	4
Step change *Vref*	T_r (ms)	FL	1.5	0.7
		10% of FL	1.7	0.9
	VDF (%)	FL	0	0
		10% of FL	3	2.5
Step change *Vi*	T_r (ms)	FL	2.5	1.1
	VDF (%)	FL	7.7	6
Robustness against step change in R_o			Yes	Yes
Robustness against step change in L_r			Yes	Yes
Robustness against step change in V_{ref}			Yes	Yes
Robustness against step change in V_i			Yes	Yes

6.5. OVERVIEW OF PUBLICATION III

In this section, different issues of the publication presented in chapter 4 are presented including a discussion on the objectives, proposed solution, most significant contributions and main results.

6.5.1 OBJECTIVES

The purpose of this publication is to present a proper control scheme for a multiple-output DC/DC class-D CSPRC. As in previous cases, the control objectives are regulating output voltages and ensuring ZVS condition.

6.5.2 PROPOSED SOLUTION

A cascaded control configuration is proposed to this end, including an outer voltage loop and an inner current loop. ZVS conditions are guaranteed by driving the switches with a robust amplitude modulation technique. The control scheme is responsible for both

Table. 6.7. Static result of the proposed control method in Publication III

L_m(µH)	Δv_o (V)	f_{min} (kHz)	f_{max} (kHz)	v_c (V)				ZVS
				up		down		
				max	min	max	min	
5.3	0	f_r	f_r	22	18	-18	-22	√
20	0	f_r	f_r	23	13	-13	-23	√

regulating the output voltage and providing zero voltage switching (ZVS) conditions in all different operating conditions including load step changes or resonant parameter variations.

6.5.3. CONTRIBUTIONS

In order to charge electric devices such as laptop PC and smart phone or other electronic loads without using AC adapters, a simple and low cost DC/DC converter using a multi-output current source resonant converter is proposed. As an example, a three output regulator is considered in this study in which three level voltages of 5V, 9V and 12V are simultaneously provided. Theoretical analysis includes the derivation of the averaged large-signal model and the synthesis of the control scheme.

6.5.4. ANALYSIS OF THE RESULTS

In chapter 4, the SMC control scheme presented in publication II is extended to be used in an application of multiple-output CSPRC. So this section covers the analysis of the benefits of SMC control in this new developed control scheme.

To verify the effectiveness of the developed control schemes, their static and dynamic properties are analyzed. Table 6.7 shows the analysis results of some static parameters such as voltage regulation, range of switching frequency, amplitude of the resonant voltage and ZVS condition.

As can be seen, the resonant inverter is always tracking the resonant frequency f_r and ZVS condition is always guaranteed for different resonant inductor parameters proving the

Table. 6.8. Dynamic result of the proposed control method in Publication III

R1	R2	R3	T_r (ms)			VDF (%)		
			Vo1	*Vo2*	*Vo3*	*Vo1*	*Vo2*	*Vo3*
FL --> 10%FL	FL	FL	7	7	7	1	1.5	2
10%FL	FL --> 10%FL	FL	9	9	9	1.25	1.75	2.5
10%FL	10%FL	FL --> 10%FL	11	11	11	2	2.5	3.5
10%FL --> FL	10%FL	10%FL	7	7	7	1	1.5	2
FL	10%FL --> FL	10%FL	9	9	9	1.25	1.75	2.5
FL	FL	10%FL --> FL	11	11	11	2	2.5	3.5

robustness of the proposed control scheme. However, there is a variation of about 6 V in the amplitude of the resonant capacitor voltage in steady-state.

Table 6.8 summarizes some detail data about transient time T_r and voltage deviation in load side for different load conditions. Note that the most significant voltage deviation and settling time (3.5% and 11ms, respectively) is obtained when R3 is changed from FL to its 10% of FL or vice versa due to its higher voltage value.

6.6. OVERVIEW OF PUBLICATION IV

Control objectives, proposed solution, most significant contributions and analysis of the obtained results of the last publication is presented in this section.

6.6.1 OBJECTIVES

In this publication, a robust control method for a CSRC is proposed 1) to provide a constant output voltage, 2) to track the resonant frequency, and 3) to ensure ZVS condition, regardless of any changes in system parameters or/and load variations.

6.6.2 PROPOSED SOLUTION

The proposed method is based on a simple primary-side controller for governing the input power and a secondary-side sliding mode controller based on amplitude modulation technique to regulate the output voltage. Note that ZVS operation is guaranteed in voltages of both sides of the transformer.

Table. 6.9. Static result of the proposed control method in Publication IV

$R_o(\Omega)$	L_g (mm)	Δv_o (V)	f_{min} (kHz)	f_{max} (kHz)	V_s (V)				ZVS
					up		down		
					max	min	max	min	
20	5	0	f_r	f_r	320	300	-300	-320	√
200	5	0	f_r	f_r	330	270	-270	-330	√
20	50	0	f_r	f_r	215	210	-210	-215	√
200	50	0	f_r	f_r	200	260	-180	-280	√

6.6.3. CONTRIBUTIONS

In this method, unlike the conventional wireless energy transfer systems, there is no need to use neither a wireless communication system nor mutual coupling estimation. The reason is that the control system of each converter in both sides of transformer only uses data measured from their own sides.

6.6.4. ANALYSIS OF THE RESULTS

In Section 5, the control method proposed in the publication II is used. In this case, the original control scheme has been modified and adapted to be used in an application of wireless energy transfer system with variable air gap. So this section covers the analysis of the benefits of SMC control in this application.

The effectiveness of the proposed control scheme in the last publication is validated through analyzing its static and dynamic properties. Table 6.9 contains the static results obtained from different operation conditions, i.e., different combination of the load value and air-gap length. Same as previous SMC control schemes in this thesis, the control provides a good output voltage regulation and ensures ZVS condition in all combinations. Furthermore, the converter is working in resonant frequency. However, there is an amplitude variation in secondary side resonant voltage v_s. Note that, by changing the load from FL to

Table. 6.10. Dynamic result of the proposed control method in Publication IV

Ro	T_r (ms)	VDF (%)
FL --> 10%FL	10	7.3
10%FL --> FL	12	5

10% of FL, this amplitude variation increases. In addition, as air gap length is lower, the amplitude variation is higher.

Table 6.10 shows dynamic results shown in the last publication. This results proves the effectiveness of the proposed SMC control scheme presented for this particular application.

6.6. CONCLUSION

To sum up, it can be concluded that:

- Compared to frequency modulation control, the SMC control provides slightly better transient response and voltage deviation. However, both control methods are robust against the parameter variations including changes in the input voltage, output reference voltage and even in resonant circuit parameters.
- The best and fast transient response can be achieved by the Class-D CSPRC with two control actions or the advanced control scheme proposed in Publication II. However, adding a new switch reduces the efficiency of the system.
- In the SMC control scheme, the resonant voltage is suffering from a variation in amplitude in steady-state which may limit its practical use in some applications.
- In frequency modulation control, the transient response of the control is not much fast as in SMC control, but the resonant capacitor voltage amplitude is constant in steady-state.
- The control schemes developed for two applications of multiple-output CSPRC and WPT, provide all the benefits mentioned for the SMC.

CHAPTER 7

Conclusions and future work

Summary

This chapter presents the most relevant conclusions obtained in the development of the thesis, and presents the future works that can be investigated to continue the outline initiated in this work.

7.1. CONCLUSION

This thesis addresses the control methods applied to current source resonant converters, especially in two different applications of DC-DC and wireless power transfer system.

In the introduction of this thesis, the state-of-the-art and current researches dealing with resonant converters have been presented. Also, a classification for the resonant converter applications are introduced according to the different types of input source, resonant tank and voltage sink. In fact, the existing applications are mostly working with voltage source. As mentioned, for voltage-source resonant converters, many control strategies have been analyzed and investigated, turning this into a mature technology nowadays. Hence, there is an obvious lack of control methods applicable to current source resonant converters. The objectives of this thesis are used to fill this gap. To achieve this goal, this thesis proposes two control methods, i.e., the frequency modulation control scheme presented in publication I and the sliding mode control scheme presented in Publication II.

The results show that sliding mode control provides slightly better transient response and voltage deviation. However, in majority of the cases, both control methods are robust against any disturbance including step changes in input voltage, output reference voltage and even in resonant circuit parameters. So, it can be concluded that both control schemes ensure all the control objectives. So it is not easy to state which one is the best. Actually, both have some benefits and drawbacks. For example, in SMC control scheme, the resonant voltage is suffering from a variation in amplitude in steady-state which may limit its practical use in some applications. In contrary, in frequency modulation control, the transient response of the control is not much fast as in SMC control, but the resonant capacitor voltage amplitude is constant. So, depending on the application, one of these two control schemes can be used.

The benefits of the proposed sliding mode control have been analyzed for two different applications of multiple-output power switching supply (Publication III) and wireless power transfer system (Publication IV). Both static and dynamic results prove the effectiveness of the proposed sliding mode controls in these applications by satisfying all the aforementioned control objectives.

7.2. FUTURE WORKS

Some possible future works related to this thesis are summarized in the following points:

- *Analysis the effect of different resonant tank configurations*: This thesis addressed the current source resonant converter with a LC parallel resonant circuit topology in Publications I, II, and III and a complex five-order resonant tank in Publication IV. As we know, other configurations such as three or four elements resonant topologies could be implemented in resonant tank especially for the first three publications. The analysis of these configurations on converters with multiple output could be considered for future works.

- *Analysis of a wireless power transfer system with multiple-output:* In this thesis, only a single output wireless power transfer system was studied. But there are many challengeable problems to solve in WPT systems with multiple outputs. So one of the open topics of this thesis is working in these applications with multiple-output.

- *Prototype*: Only a low power prototype has been implemented to validate the theoretical predictions of a class-D current source parallel resonant converter. It could be interesting to realize a medium or high power current source resonant converter.

- *Analyzing the usage of current source resonant converters in other applications:* In this thesis, two applications of power supply and WPT system were considered. It could be interesting to analyze the effect of these converters in other applications. For instance, recently, inductive contactless energy transfer system in residential area has been gaining more and more success and reputation in industry and academic area. So, this application is strongly recommended due to its future widespread use.

BIBLIOGRAPHY

[1] R. P. Severns and G Bloom, *Modern DC-to-DC Switch-mode Power Converter Circuits,* New York: Van Nostrand Reinhold, 1985.

[2] J. G Kassakian, M. S. Schlecht, and G C. Verghese, *Principles of Power Electronics,* Reading, MA: Addison-Wesley, 1991.

[3] N. Mohan, T. M. Undeland, and W. P. Robbins, *Power Electronics: Converters, Applications and Design,* 3rd Ed. Hoboken, NJ: John Wiley & Sons, 2003.

[4] I. Batarseh, *Power Electronic Circuits,* Hoboken, NJ: John Wiley & Sons, 2004.

[5] M. K. Kazimierczuk, *Pulse-Width Modulated DC-DC Power Converters,* Chichester, UK: John Wiley & Sons, 2008.

[6] R. Li, D. Xu, B. Feng, K. Mino, and H. Umida, "Efficiency and EMI analysis for a ZVS-SVM controlled three-phase boost PFC converter," in *Proc. 22nd IEEE Appl. Power Electron. Annu. Conf. (APEC),* 2007, pp. 1351–1355.

[7] S. Hrigua, F. Costa, C. Gautier, and B. Revol, "New method of EMI analysis in power electronics based on semiconductors transient models: Application to SiC MOSFET/ Schottky diode," in *Proc. 38th IEEE Ind. Electron. Soc. Annu. Conf. (IECON),* 2012, pp. 590–595.

[8] Y. Yang, D. Huang, F. C. Lee, and Q. Li, "Analysis and reduction of common mode EMI noise for resonant converters," in *Proc. 29th Annu. IEEE Appl. Power Electron. Conf. and Expo. (APEC),* 2014, pp. 566–571.

[9] N. Sudhakar, N. Rajasekar, V. T. Rohit, E. Rakesh, and J. Jacob, "EMI mitigation in closed loop boost converter using soft switching combined with chaotic mapping," in *Proc. Int. Conf. Advances Elect. Eng. (ICAEE),* 2014, pp. 1–6.

[10] S. Bansala and L. M. Saini, "Analysis and comparison of various soft switching topologies for PSFB DC-DC converter with additional auxiliary circuits," *Int. Elect. Eng. J. (IEEJ),* vol. 5, no. 2, pp. 1255–1268, 2014.

[11] S. Y. Hui and H. S. H. Chung, "Resonant and Soft-Switching Converters," in *Power Electronics Handbook,* 2nd ed., M. H. Rashid, Ed. Burlington, MA: Academic, 2007, pp. 405–449.

[12] Wei Tang, Ching-Shan Leu and F. C. Lee, "Charge control for zero-voltage-switching multiresonant converter," in *IEEE Transactions on Power Electronics*, vol. 11, no. 2, pp. 270-274, Mar 1996.

[13] D. Maksimovic and S. Cuk, "A general approach to synthesis and analysis of quasi-resonant converters," *IEEE Trans. Power Electron.,* vol. 6, no. 1, pp. 127–140, Jan. 1991.

[14] Y. S. Noh, M. S. Oh, M. Y. Ryu, J. Kim, and C. Y. Won, "Isolated bi-directional DC/DC converter using quasi-resonant ZVS," in *Proc. 2014 IEEE Int. Conf. Ind. Technol. (ICIT),* 2014, pp. 514–518.

[15] S. Chudjuarjeen, V. Hathairatsiri, W. Pechpunsri, A. Sangswang, and C. Koompai, “Quasiresonant converter for induction heating in high temperature applications,” in *Proc. 10th IEEE Int. Conf. Power Electron. and Drive Syst. (PEDS)*, 2013, pp. 836–839.

[16] O. A. Pop, “Analysis and simulation of quasiresonant inverter for induction heating applications,” in *Proc. 49th Int. Universities Power Eng. Conf. (UPEC)*, 2014, pp. 1–4.

[17] M. L. Martins, J. L. Russi, and H. L. Hey, “Low reactive energy ZCZVT PWM converters: Synthesis, analysis and comparison,” in *Proc. 36th IEEE Power Electron. Specialists Conf. (PESC)*, 2005, pp. 1234–1240.

[18] V. Tuomainen and J. Kyyra, “Effect of resonant transition on efficiency of forward converter with active clamp and self-driven SRs,” *IEEE Trans. Power Electron.*, vol. 20, no. 2, pp. 315–323, 2005.

[19] M. T. Outeiro, G. Buja and D. Czarkowski, "Resonant Power Converters: An Overview with Multiple Elements in the Resonant Tank Network," in *IEEE Industrial Electronics Magazine*, vol. 10, no. 2, pp. 21-45, June 2016.

[20] I. Batarseh, “Resonant converter topologies with three and four energy storage elements,” *IEEE Trans. Power Electron.*, vol. 9, no. 1, pp. 64–73, Jan. 1994.

[21] S. Tian, F. C. Lee and Q. Li, "A Simplified Equivalent Circuit Model of Series Resonant Converter," in *IEEE Transactions on Power Electronics*, vol. 31, no. 5, pp. 3922-3931, May 2016.

[22] H. Molla-Ahmadian, F. Tahami, A. Karimpour, and N. Pariz, “Hybrid control of DC-DC series resonant converters: The direct piecewise affine approach,” *IEEE Trans. Power Electron.*, vol. 30, no. 3, pp. 1714–1723, Mar. 2015.

[23] M. K. Kazimierczuk and D. Czarkowski, “Resonant Power Converters”, Wiley-Interscience, 1995.

[24] A. Momeneh, M. Castilla, F. F. A. van der Pijl, M. Moradi and J. Torres, "New Inductive Contactless Energy Transfer System For Residential Distribution Networks With Multiple Mobile Loads," *2015 17th European Conference on Power Electronics and Applications (EPE'15 ECCE-Europe)*, Geneva, 2015, pp. 1-10.

[25] J. Deng, C. C. Mi, R. Ma and S. Li, "Design of LLC Resonant Converters Based on Operation-Mode Analysis for Level Two PHEV Battery Chargers," in *IEEE/ASME Transactions on Mechatronics*, vol. 20, no. 4, pp. 1595-1606, Aug. 2015.

[26] J. L. Sosa, M. Castilla, J. Miret, L. García de Vicuna, and J. Matas, ˜ “Modeling and performance analysis of the DC/DC series–parallel resonant converter operating with discrete self-sustained phase-shift modulation technique,” *IEEE Trans. Ind. Electron.*, vol. 56, no. 3, pp. 697–705, Mar. 2009.

[27] M. Castilla, L. García de Vicuna, M. López, O. López, and J. Matas, “On the design of sliding mode control schemes for quantum resonant converters,” *IEEE Trans. Power Electron.*, vol. 15, no. 6, pp. 960–973, Nov. 2000.

[28] L. García de Vicuna, M. Castilla, J. Miret, J. Matas, and J. M. Guerrero, “Sliding-mode control for a single-phase AC/AC quantum resonant converter,” *IEEE Trans. Ind. Electron.*, vol. 56, no. 9, pp. 3496–3504, Sep. 2009.

[29] M. Kazimierczuk and M. Jutty, "Fixed-frequency phase controlled full bridge resonant converter with a series load," IEEE Trans. Power Electron., vol. 10, no. 1, pp. 9-18, January 1995.

[30] H. Sheng, D. Fu, X. Yang, F. Wang and F. Lee, "Comparison of ZVS operation modes with and without phase shift for three-level resonant converters," IEEE Applied Power Electronics Conference Proc., 2006.

[31] A. K. S. Bhat, "A fixed frequency modified series resonant converter: analysis, design and experimental results," IEEE Trans. Power Electron., vol. 10, no. 6, pp. 766-775, November 1995.

[32] M. Z. Youssef and P. K. Jain, "Series–parallel resonant converter in selfsustained oscillation mode with the high-frequency transformer-leakageinductance effect: analysis, modeling, and design," IEEE Trans. Ind. Electron., vol. 54, no. 3, pp. 1329-1341, June 2007.

[33] A. P. Hu, G. A. Covic, and J. T. Boys, “Direct ZVS start-up of a current fed resonant inverter,” *IEEE Trans. Power Electron.*, vol. 21, no. 3, pp. 809–812, May 2006.

[34] A. Namadmalan and J. S. Moghani, “Self-oscillating switching technique for current source parallel resonant induction heating systems,” *J. Power Electron.*, vol. 12, no. 6, pp. 851–858, Nov. 2012.

[35] A. Namadmalan and J. S. Moghani, “Tunable self-oscillating switching technique for current source induction heating systems,” *IEEE Trans. Power Electron.*, vol. 61, no. 5, pp. 2556–2563, May 2014.

[36] A. Namadmalan, “Bidirectional current fed resonant inverter for contactless energy transfer systems,” *IEEE Trans. Ind. Electron.*, vol. 62, no. 1, pp. 238–245, Jan. 2015.

[37] H. Koizumi, “A delta-sigma modulated class-D current-source resonant boost converter,” in *Proc. Annu. meeting IEEE Ind. Electron. Soc.*, 2010, pp. 269–273.

[38] M. T. Outeiro, G. Buja, and A. Carvalho, “Resonant converters for electric equipment power supply,” in *Proc. 40th IEEE Ind. Electron. Soc. Annu. Conf. (IECON)*, 2014, pp. 5065–5071.

[39] S. M. Mousavi, R. Beiranvand, S. Goodarzi, and M. Mohamadian, “Designing a 48 V to 24 V DCDC converter for vehicle application using a resonant switched capacitor converter topology,” in *Proc. 6th Power Electron., Drive Syst., and Technol. Conf. (PEDSTC)*, 2015, pp. 263–268.

[40] N. Shafiei, M. Ordonez, M. Craciun, C. Botting, and M. Edington, “Burst mode elimination in high-power resonant battery charger for electric vehicles,” *IEEE Trans. Power Electron.*, vol. 31, no. 2, pp. 1173–1188, 2016.

[41] D. Moon, J. Park, and S. Choi, “New interleaved current-fed resonant converter with significantly reduced high current side output filter for EV and HEV applications,” *IEEE Trans. Power Electron.*, vol. 30, no. 8, pp. 4264– 4271, 2015.

[42] E.Asa, K.Colak, M.Bojarski, and D.Czarkowski, “A novel phase control of semi bridgeless active rectifier for wireless power transfer applications,” in *Proc. IEEE Appl. Power Electron. Conf. and Expo. (APEC)*, 2015, pp. 3225–3231.

[43] M. Bojarski, E. Asa, M. T. Outeiro, and D. Czarkowski, “Control and analysis of multi-level type multi-phase resonant converter for wireless EV charging” in *40th IEEE Ind. Electron. Soc. Annu. Conf. (IECON)*, 2015, pp. 5065–5071.

[44] S. Samanta and A. K. Rathore, “A new current-fed (C) (LC) (LC) topology for inductive wireless power transfer (IWPT) application: Analysis, design, and experimental results,” in *Proc. IEEE Energy Conversion Congr. and Expo. (ECCE)*, 2015, pp. 1279–1285.

[45] D. S. Gautam and A. K. S. Bhat, “A comparison of soft-switched DC-to-DC converters for electrolyzer application,” *IEEE Trans. Power Electron.*, vol. 28, no. 1, pp. 54–63, 2013.

[46] M. A. Rezaei, K. J. Lee, and A. Q. Huang, “A high-efficiency flyback micro-inverter with a new adaptive snubber for photovoltaic applications,” *IEEE Trans. Power Electron.*, vol. 31, no. 1, pp. 318–327, 2016.

[47] M. T. Outeiro and A. S. Carvalho, “Methodology of designing power converters for fuel cell based systems: A resonant approach,” in *New Developments in Renewable Energies*, H. Arman and I. Yuksel, Eds. Rijeka. Croatia: InTech, 2013.

[48] M. T. Outeiro and A. Carvalho, “Design, implementation and experimental validation of a DC-DC resonant converter for PEM fuel cell applications,” in *Proc. 39th IEEE Ind. Electron. Soc. Annu. Conf. (IECON)*, 2013, pp. 619–624.

[49] W. Chen, X. Wu, L. Yao, W. Jiang, and R. Hu, “A step-up resonant converter for grid-connected renewable energy sources,” *IEEE Trans. Power Electron.*, vol. 30, no. 6, pp. 3017–2039, June 2015.

[50] R. N. Beres, X. Wang, F. Blaabjerg, M. Liserre, and C. L. Bak, “Optimal design of high-order passive-damped filters for grid-connected applications,” *IEEE Trans. Power Electron.*, vol. 31, no. 3, pp. 2083–2098, Mar. 2016.

[51] T. Mishima, Y. Nakagawa, and M. Nakaoka, “A bridgeless BHB ZVS-PWM AC-AC converter for high-frequency induction heating applications,” *IEEE Trans. Ind. Appl.*, vol. 51, no. 4, pp. 3304–3315, 2015.

[52] H. Sarnago, O. Lucía, A. Mediano, and J. M. Burdío, “Multi-MOSFET-based series resonant inverter for improved efficiency and power density induction heating applications,” *IEEE Trans. Power Electron.*, vol. 29, no. 8, pp. 4301– 4312, Aug. 2014.

[53] H. Sarnago, O. Lucia, A. Mediano, and J. M. Burdio, “Design and implementation of a high-efficiency multiple-output resonant converter for induction heating applications featuring wide bandgap devices,” *IEEE Trans. Power Electron.*, vol. 29, no. 5, pp. 2539–2549, May 2014.

[54] X. Zhang, T. C. Green, and A. Junyent-Ferre, “A new resonant modular ´multilevel step-down DC–DC converter with inherent-balancing,” *IEEE Trans. Power Electron.*, vol. 30, no. 1, pp. 78–88, Jan. 2015.

[55] D. Reusch and J. Strydom, “Evaluation of gallium nitride transistors in high frequency resonant and soft-switching DC–DC converters,” *IEEE Trans. Power Electron.*, vol. 30, no. 9, pp. 5151–5158, Sep. 2015.

[56] J. T. Boys, G. A. Covic, and A. W. Green, “Stability and control of inductively coupled power transfer system,” *Proc. Inst. Elect. Eng.—Elect. Power Appl.*, vol. 147, no. 1, pp. 37–43, Jan. 2000.

[57] K. C. Wan, Q. Xue, X. Liu, and S. Y. Hui, “Passive radio frequency repeater for enhancing signal reception and transmission in a wireless charging platform,” *IEEE Trans. Ind. Electron.*, vol. 61, no. 4, pp. 1750–1757, Apr. 2014.

[58] F. Musavi and W. Eberle, “Overview of wireless power transfer technologies for electric vehicle battery charging,” *IET Power Electron.*, vol. 7, no. 1, pp. 60–66, Jan. 2014.

[59] A. K. Ram-Rakhyani and G. Lazzi, “On the design of efficient multi coil telemetry system for biomedical implants,” *IEEE Trans. Biomed. Circuits Syst.*, vol. 7, no. 1, pp. 11–23, Feb. 2013.

[60] S. H. Lee, B. S. Lee and J. H. Lee, “A New Design Methodology for a 300-kW, Low Flux Density, Large Air Gap, Online Wireless Power Transfer System,” *IEEE Trans. Industry Applications*, vol. 52, no. 5, pp. 4234-4242, Sept.-Oct. 2016.

[61] K. Colak, E. Asa, M. Bojarski, D. Czarkowski and O. C. Onar, “A Novel Phase-Shift Control of Semibridgeless Active Rectifier for Wireless Power Transfer,” *IEEE Trans. Power Electronics*, vol. 30, no. 11, pp. 6288-6297, Nov. 2015.

[62] J. Tian and A. P. Hu, "A DC-Voltage-Controlled Variable Capacitor for Stabilizing the ZVS Frequency of a Resonant Converter for Wireless Power Transfer," *IEEE Trans. Power Electronics*, vol. 32, no. 3, pp. 2312- 2318, March 2017.

[63] S. Judek, "Control system for contactless electrical energy transfer with varying air gap," 2014 *International Conference on Applied Electronics, Pilsen*, 2014, pp. 149-152.

[64] S. Judek and K. Karwowski, "Analysis of inductive power transfer systems for variable air gap and voltage supply frequency," *IEEE International Symposium on Industrial Electronics*, Gdansk, 2011, pp. 1963-1968.

[65] C. Liu, A. P. Hu, B. Wang, and N. C. Nair, “A capacitively coupled contactless matrix charging platform with soft switched transformer control,” *IEEE Trans. Ind. Electron.*, vol. 60, no. 1, pp. 249–260, Jan. 2013.

[66] J. E. James, D. R. Robertson, and G. A. Covic, “Improved AC pickups for IPT systems,” *IEEE Trans. Power Electron.*, vol. 29, no. 12, pp. 6361–6374, Dec. 2014.

[67] N. Y. Kim, K. Y. Kim, J. Choi, and C. W. Kim, “Adaptive frequency with power-level tracking system for efficient magnetic resonance wireless power transfer,” *Electron. Lett.*, vol. 48, no. 8, pp. 452–454, Apr. 2012.

[68] J. Miller, O. Onar, and M. Chinthavali, “Primary-side power flow control of wireless power transfer for electric vehicle charging,” *IEEE J. Emerg. Sel. Topics Power Electron.*, vol. 3, no. 1, pp. 147–162, Mar. 2015.

[69] S. Y. R. Hui, D. Lin, J. Yin, and C. K. Lee, “Method for parameter identification, load monitoring and output power control of wireless power transfer systems,” U.S. Patent application, US 61/862,627, Aug. 6, 2013.

[70] S. R. Sanders and G. C. Verghese, "Lyapunov-Based Control For Switched Power Converters," in *IEEE Transactions on Power Electronics*, vol. 7, no. 1, pp. 17-24, Jan 1992.

[71] A. R. Namadmalan, B. Abdi and J. S. Moghani, "Current-fed parallel resonant push-pull inverter with coil flux control for induction heating applications," *2010 1st Power Electronic & Drive Systems & Technologies Conference (PEDSTC)*, Tehran, Iran, 2010, pp. 186-190.

[72] M. Castilla, L. G. de Vicuna, M. Lopez and J. Font, "A sliding mode controller for the current-source parallel-resonant converter with zero-voltage switching," *Industrial Electronics, Control and Instrumentation, 1997. IECON 97. 23rd International Conference on*, New Orleans, LA, 1997, pp. 477-482 vol.2.

[73] X. Dai and Y. Sun, "An Accurate Frequency Tracking Method Based on Short Current Detection for Inductive Power Transfer System," *in IEEE Transactions on Industrial Electronics*, vol. 61, no. 2, pp. 776-783, Feb. 2014.